Science of the Total Environment 951 (2024) 175522

Contents lists available at ScienceDirect

Science of the Total Environment

journal homepage: www.elsevier.com/locate/scitotenv

Strontium isotopes in the atmosphere, geosphere and hydrosphere: Developing a systematic "fingerprinting" framework of rocks and water in sedimentary basins in eastern Australia

M. Raiber [a,b,c,*], A.J. Feitz [d], S. Flook [e], D.I. Cendón [f,g], A. Suckow [h], G. Schöning [e], H. Hofmann [a,i], J. Martinez [a,j], R. Maas [k], B.F.J. Kelly [g]

[a] CSIRO Environment, Brisbane, Queensland, Australia
[b] School of Earth, Environmental and Biological Sciences, Science & Engineering Faculty, Queensland University of Technology, Brisbane, Queensland, Australia
[c] National Centre for Groundwater Research and Training (NCGRT), Australia
[d] Geoscience Australia, Canberra, Australian Capital Territory, Australia
[e] Office of Groundwater Impact Assessment (OGIA), Department of Regional Development, Manufacturing and Water, Brisbane, Queensland, Australia
[f] Australian Nuclear Science and Technology Organisation (ANSTO), Lucas Heights, New South Wales, Australia
[g] School of Biological, Earth and Environmental Sciences, University of New South Wales, Sydney, Australia
[h] CSIRO Environment, Adelaide, South Australia, Australia
[i] School of the Environment, University of Queensland, Brisbane, Australia
[j] Eco Logical Australia, Brisbane, Queensland, Australia
[k] School of Geography, Earth and Atmospheric Sciences (SGEAS), University of Melbourne, Victoria, Australia

HIGHLIGHTS

- Development of $^{87}Sr/^{86}Sr$ fingerprinting framework in eastern Australian sedimentary basins
- Analysis of $^{87}Sr/^{86}Sr$ of rocks, groundwater, surface water and rainfall
- Major hydrogeological units have narrow $^{87}Sr/^{86}Sr$ population characteristics.
- Comparison of $^{87}Sr/^{86}Sr$ and ^{14}C and ^{36}Cl shows that $^{87}Sr/^{86}Sr$ is established early along flow path.
- $^{87}Sr/^{86}Sr$ confirmed as a powerful chemo- and hydrostratigraphic fingerprinting tool.

GRAPHICAL ABSTRACT

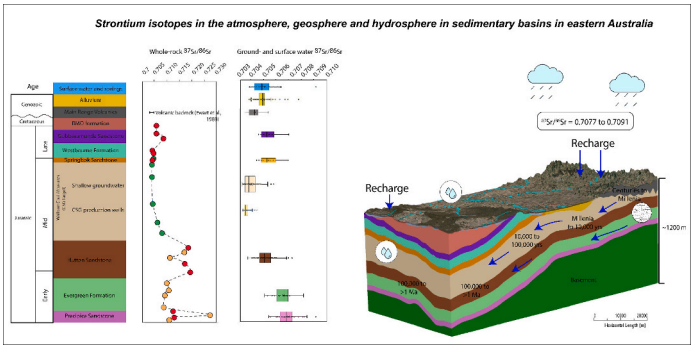

ARTICLE INFO

Editor: Christian Herrera

Keywords:
Strontium isotopes
Aquifer connection
Groundwater-dependent ecosystems (GDEs)

ABSTRACT

Understanding the connection between aquifers, aquitards, and groundwater-dependant ecosystems remains a key challenge when developing a conceptual hydrogeological model. The aim of this study was to develop a systematic strontium isotope ($^{87}Sr/^{86}Sr$) fingerprinting framework of rocks and water within the sedimentary Surat and Clarence-Moreton basins (SCM basins) in eastern Australia – an area of extensive coal seam gas development and high potential for aquifer and groundwater-surface water connectivity. To do this, new groundwater samples ($n = 298$) were collected, analyzed and integrated with published data ($n = 154$) from the

* Corresponding author at: CSIRO Environment, Brisbane, Queensland, Australia.
E-mail address: Matthias.Raiber@csiro.au (M. Raiber).

https://doi.org/10.1016/j.scitotenv.2024.175522
Received 16 May 2024; Received in revised form 12 August 2024; Accepted 12 August 2024
Available online 14 August 2024

Surat Basin
Clarence-Moreton Basin
Great Artesian Basin (GAB)

basins' major sedimentary, volcanic and alluvial aquifers, including the major coal seam gas target, the Walloon Coal Measures. Samples were also analyzed from rainfall ($n = 2$) and surface water ($n = 40$). In addition, rock core samples ($n = 39$) from exploration and stratigraphic wells were analyzed to determine the range of Sr isotope composition from host rocks. The analyses of cores demonstrate a distinct and systematic contrast in $^{87}Sr/^{86}Sr$ between different hydrogeological units. This confirms that all major hydrogeological units have a narrow range with unique $^{87}Sr/^{86}Sr$ population characteristics that are useful for guiding conceptual model development. Comparison with selected hydrochemical and groundwater age tracers (^{14}C and ^{36}Cl) suggests only limited changes of $^{87}Sr/^{86}Sr$ from recharge beds to the deeper parts of the basins or with a decrease in natural ^{14}C and ^{36}Cl tracer content along flow paths. Stream sampling during baseflow conditions confirms that $^{87}Sr/^{86}Sr$ in surface waters are similar to those of the underlying bedrock formations. We demonstrated that $^{87}Sr/^{86}Sr$ analyses of rocks and water provide a powerful hydrostratigraphic and chemostratigraphic fingerprinting framework in the SCM basins, enabling reliable assessments of plausible aquifer and groundwater-surface water interconnectivity pathways. Applied in other complex multi-aquifer sedimentary basins in Australia, and globally, a

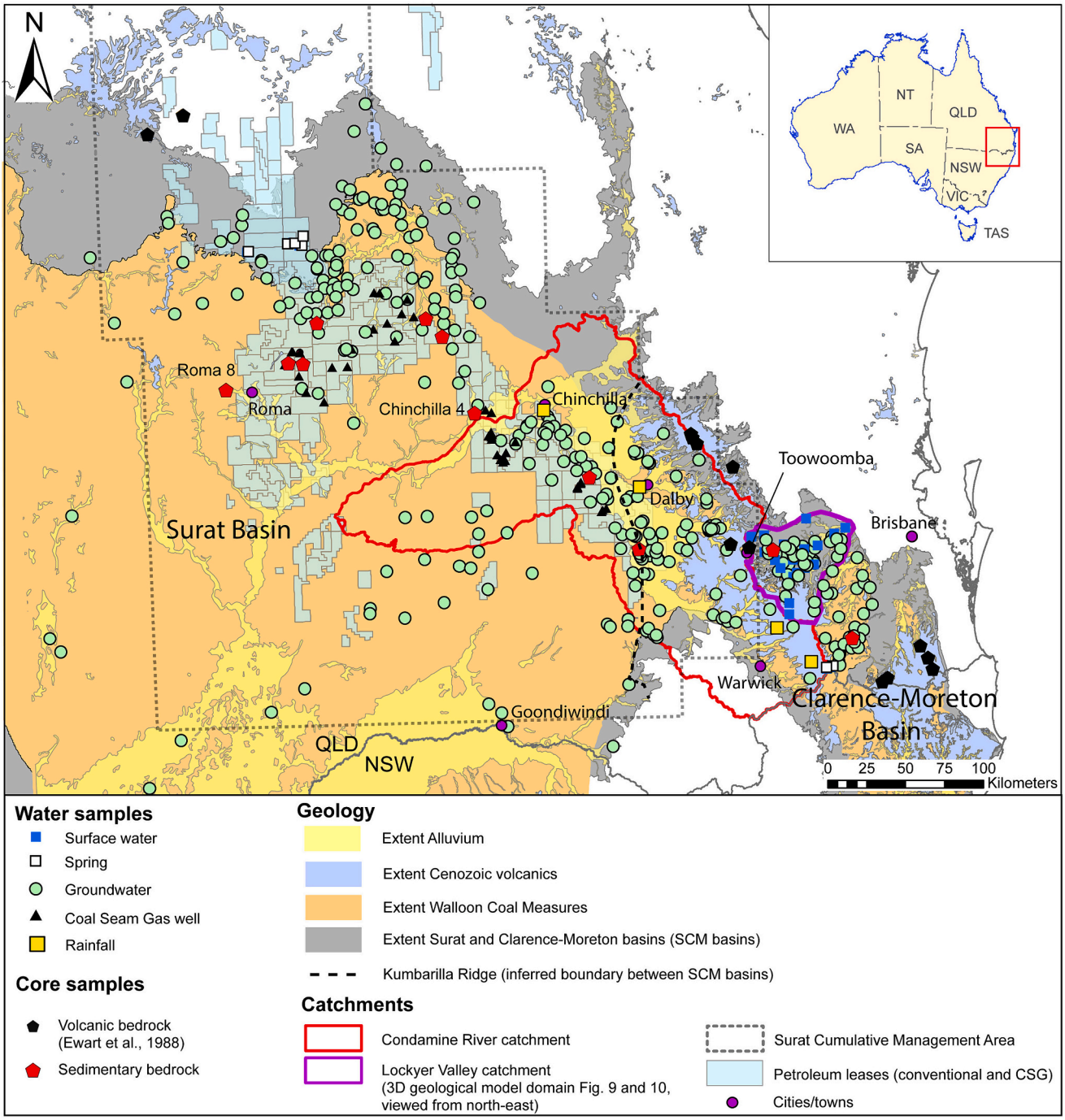

Fig. 1. Simplified surface geology and groundwater, surface water, and core sampling locations in the Surat and Clarence-Moreton basins.

similar approach can help to constrain conceptual hydrogeological models and facilitate improved water resource management.

1. Introduction

The Early Jurassic to Late Cretaceous Surat and Clarence-Moreton (SCM) basins are two large, intracratonic sedimentary basins in eastern Australia, together covering an area of >370,000 km^2 (Fig. 1). These basins host sequences of aquifers and aquitards including the Walloon Coal Measures, which contain economic coal and coal seam gas (CSG) resources. Increasing CSG production from the Surat Basin and the Bowen Basin (Fig. 1) resulted in Australia becoming one of the major global producers of CSG (Li et al., 2018). At the same time, these basins include large aquifers, which form part of the Great Artesian Basin (GAB), with some of the deeper aquifers also investigated as carbon capture and storage (CCS) sites (Bradshaw et al., 2009; Hofmann et al., 2024). Partially overlying the SCM basins are extensive late Paleogene to early Neogene volcanic systems (e.g. Main Range Volcanics and Lamington Volcanics) and alluvial aquifers (e.g. the Condamine and the Lockyer Valley), all of which are critical water resources to sustain agricultural activities and regulate environmentally sensitive ecosystems. For instance, approximately AUS$ 1.32 billion of agricultural commodities were produced in the Condamine River catchment in 2018–19 (ABS, 2020). Understanding how and where interactions between different aquifers (including the target CSG formation) and surface water occur in such complex hydrogeological settings with many competing water resource users is very important for water planning and management (Flook et al., 2020; Pandey et al., 2020).

Many techniques are commonly used to determine hydraulic connections between aquifers and surface water, including hydrochemistry, environmental tracers, geophysical techniques, and modelling (e.g. Flook et al., 2020; Iverach et al., 2015; Raiber et al., 2019). One isotopic tracer often applied is the strontium isotope ratio ($^{87}Sr/^{86}Sr$). Decay of the natural long-lived rubidium isotope (^{87}Rb) with a half-life of 4.967 $\times$ 10^{10} years (Kossert, 2003) forms the radiogenic (in origin) and stable isotope ^{87}Sr, which is compared to its stable counterpart ^{86}Sr. Generally, $^{87}Sr/^{86}Sr$ in terrestrial environments is controlled by water–rock interactions and water–mass mixing (McNutt, 2000; Faure and Powell, 2012). Low groundwater $^{87}Sr/^{86}Sr$ (~0.701 to 0.704) is typically associated with interaction of water with igneous basaltic materials (e.g. Jackson and Hart, 2006). Modern seawater and derived rain near the coast generally have $^{87}Sr/^{86}Sr$ of approximately 0.709 (e.g. Herut et al., 1993; Négrel et al., 2007; Palmer and Edmond, 1989; Raiber et al., 2009; Veizer, 1989), whereas waters interacting with granitic igneous rocks tend to have higher $^{87}Sr/^{86}Sr$ due to accumulation of Rb and long-term decay (e.g. Négrel et al., 2001).

The $^{87}Sr/^{86}Sr$ in groundwaters is primarily controlled by transfer of Sr and Sr isotopic signatures from minerals within aquifer host rocks during water-rock interaction (Petelet-Giraud et al., 2018). Groundwater $^{87}Sr/^{86}Sr$ can thus be used to trace the sources of solutes (Bagheri et al., 2014; Harrington and Herczeg, 2003) and identify interactions between aquifers (Dromagaci and Herczeg, 2002; Frost et al., 2002; Hofmann and Cartwright, 2013; King et al., 2015; Moya et al., 2016; Raiber et al., 2009) including in areas of CSG or shale gas production (Baublys et al., 2019; Chapman et al., 2012; Frost et al., 2002; Harkness et al., 2017; Hofmann et al., 2024; Lemarchand et al., 2015; OGIA, 2021a, 2023; Pearce et al., 2022).

Other applications include studies of connectivity between shallow groundwater and surface water systems (Anderson et al., 2021; Négrel et al., 2017; Petelet-Giraud et al., 2018) and the detection and tracing of anthropogenic contamination of aquifers (Neymark et al., 2018). Finally, Sr isotopes are increasingly used for tracing the geographic origin of biological materials in environmental, agricultural provenance, forensic and archaeological studies. Many of these isotopic tracing applications require an understanding of the spatial variability of $^{87}Sr/^{86}Sr$ in the geosphere, hydrosphere and biosphere (Adams et al., 2019; Bataille et al., 2018, 2020; de Caritat et al., 2022).

Strontium isotope tracing has been used in several groundwater studies in the Surat Basin and other parts of the GAB. For example, Horner et al. (2015) used compositional and Sr isotopic data for rock samples from a stratigraphic well and water samples from batch reactors to study the evolution of long-term CO_2–water–rock reaction pathways in low-salinity, siliciclastic reservoirs under geological CO_2 storage conditions. Baublys et al. (2019) used hydrochemical and Sr isotope data for CSG-produced water and its host rock (i.e. WCM) to identify water–rock interactions within gas production areas. Collerson et al. (1988) investigated $^{87}Sr/^{86}Sr$ along two inferred flow paths within the Eromanga Basin, the largest sub-basin of the GAB, located to the west of the Surat Basin (Fig. 1).

Although many studies have used $^{87}Sr/^{86}Sr$ to determine connectivity in mostly shallow and simple aquifer and/or surface water systems (e.g. with one bedrock aquifer or one alluvial aquifer and streams), very few studies have systematically assessed the $^{87}Sr/^{86}Sr$ variability of both rocks and water resources in thick and regionally extensive multi-aquifer and aquitard sequences as both a hydrostratigraphic and chemostratigraphic tool. However, using isotope fingerprinting tools to determine aquifer boundaries or hydrogeological connections between deep and shallow aquifers, between different bedrock aquifers or aquifers with surface water (e.g. streams and springs) in such complex systems requires a comprehensive understanding of all potential end-members.

In this investigation, we combine existing $^{87}Sr/^{86}Sr$ data with 295 new groundwater samples and 37 new rock samples to 1) systematically "fingerprint" rock and groundwater $^{87}Sr/^{86}Sr$ of the major hydrostratigraphic formations within the SCM basins and the overlying Cenozoic volcanic (Main Range Volcanics) and alluvial aquifers, representing the most comprehensive and systematic Sr isotope assessment completed in the GAB; 2) assess if $^{87}Sr/^{86}Sr$ can be used as a fingerprinting framework to characterize connectivity in these complex multi-aquifer systems; 3) determine if the Sr isotopes of rocks and groundwater can be used as a chemostratigraphic tool to refine hydro stratigraphy in these sedimentary basins and 4) by selecting one of the major agricultural surface water sub-catchments (Lockyer Valley) within the SCM basins, explore whether $^{87}Sr/^{86}Sr$ of groundwater and rocks of major hydrostratigraphic formations can assist in the identification of source aquifers of gaining streams.

2. Hydrogeological setting

The Clarence-Moreton Basin (CMB) covers approximately 45,000 km^2 of south-eastern Queensland and north-eastern New South Wales and extends off-shore over an area of at least 1000 km^2 in New South Wales. The adjoining Surat Basin covers approximately 327,000 km^2 in central southern Queensland and central northern New South Wales (La Croix et al., 2019). The formation of the SCM basins is closely related to large-scale tectonic processes associated with the development of the New England Orogen and the reorganization of tectonic plates which began in the Late Carboniferous (Korsch et al., 1989).

The SCM basins are bounded by exposed Palaeozoic basement blocks, which are part of the New England Orogen, and which provided the main clastic input into the SCM basins during the Early Jurassic (La Croix et al., 2020). The Surat Basin partly overlies the Bowen and Gunnedah basins, two Permian–Triassic sedimentary basins containing major economic coal deposits. Elsewhere, the SCM basins rest unconformably on basement rocks composed of metasedimentary and

metavolcanic rocks of Early Palaeozoic to Permian age, as well as granitoids emplaced from the Late Permian to the Early Triassic (Donchak et al., 2007).

The generalized stratigraphic sub-division of the SCM basins is shown in Fig. 2. This figure highlights that the Early to Mid-Jurassic sedimentary sequences are continuous across the basins, although the stratigraphic nomenclature differs. During the Early Jurassic, deposition was mostly fluvio-lacustrine, depositing the sedimentary sequences of the Precipice Sandstone and its CMB stratigraphic equivalent (Woogaroo Subgroup) (Fig. 2). The Precipice Sandstone contains a large volume of poorly cemented quartz-rich sand grains derived from erosion of the uplifted granitic basement at the margin of these basins. It was deposited by braided rivers feeding stream-dominated alluvial fans and broad plains (O'Brien and Wells, 1994) with a possible influence of marginal marine or tidal depositional environments (Martin et al., 2013). This was followed by the deposition of the low-permeability sequences of the Evergreen Formation (CMB equivalent Gatton Sandstone), composed of sequences of mudstone and argillaceous sandstone (Hayes et al., 2020), and the Hutton Sandstone (CMB equivalent Koukandowie Formation).

The upper zone of the Hutton Sandstone is characterised by relatively thick high-resistivity quartz-dominated sandstones and around clayey sandstone, siltstone and mudstone. In contrast, the lower zone is characterised by thinner shalier sandstone units and interbedded siltstones and mudstones. Cleaner and more quartzose sandstones account for <30 % of this lower zone (Bianchi et al., 2019; OGIA, 2021a, 2021b).

Combined, the Precipice Sandstone and Hutton Sandstone are the two major sedimentary bedrock aquifers used for agricultural water within the SCM basins (OGIA, 2016, 2021a; Raiber and Suckow, 2017; Smallacombe et al., 2024; Suckow et al., 2020; Vink et al., 2020). The Evergreen Formation is typically described as an aquitard, which may locally form a partial aquifer near the basin margins. Within the Evergreen Formation, the Boxvale Sandstone member forms an aquifer or partial aquifer.

The Middle Jurassic Walloon Coal Measures is the target unit for CSG exploration and development within the SCM basins. The Walloon Coal Measures is composed of volcaniclastic, lithic and silty sandstone with interbedded mudstone and siltstone (Jenkinson, 2018; Wells and O'Brien, 1994). Ash-fall tuff is also present throughout the sequence (Doig and Stanmore, 2012). The Walloon Coal Measures was deposited in low-energy fluvial-lacustrine depositional environments by highly sinuous streams meandering across a wide floodplain, as well as in shallow-water backswamps (Donchak et al., 2007; Mukherjee et al., 2021). Near the edges of the basin, deposition of channel sands was more common (Ingram and Robinson, 1996).

Overlying the Walloon Coal Measures within the Surat Basin in Queensland are multiple aquifer–aquitard sequences, most notably the Mid-Jurassic Springbok Sandstone, the Late Jurassic Gubberamunda Sandstone and the Cretaceous BMO (which includes the Bungil Formation, Mooga Sandstone and Orallo Formation) and Rolling Downs groups.

Unconformably overlying Jurassic bedrock sequences in some parts of the SCM basins are Cenozoic volcanic rocks. These are associated with large-scale volcanic migratory "swell and pinch" volcanic chains developed over intraplate plumes (Cohen et al., 2013; Sutherland, 2003). Two major eruptive centres occur in south-east Queensland (the Tweed and Focal Peak shield volcanoes) (Donchak et al., 2007). The Main Range Volcanics consist of massive, fine-grained olivine basalt, which occurs mainly as flows with minor mudstone and fine-grained sandstone locally interbedded with the flows. The lavas of the Main Range Volcanics are typically <200 m thick (Raiber et al., 2017, 2019).

Extensive alluvial sediment sequences have infilled the alluvial valleys of major streams (e.g. the Condamine River, Dawson River and Lockyer Creek) and their tributary systems (Cui et al., 2018; Martinez et al., 2015; Pandey et al., 2020; Raiber et al., 2019).

3. Methodology

3.1. Aquifer assignment

Isotopic and hydrochemical fingerprinting to infer connectivity

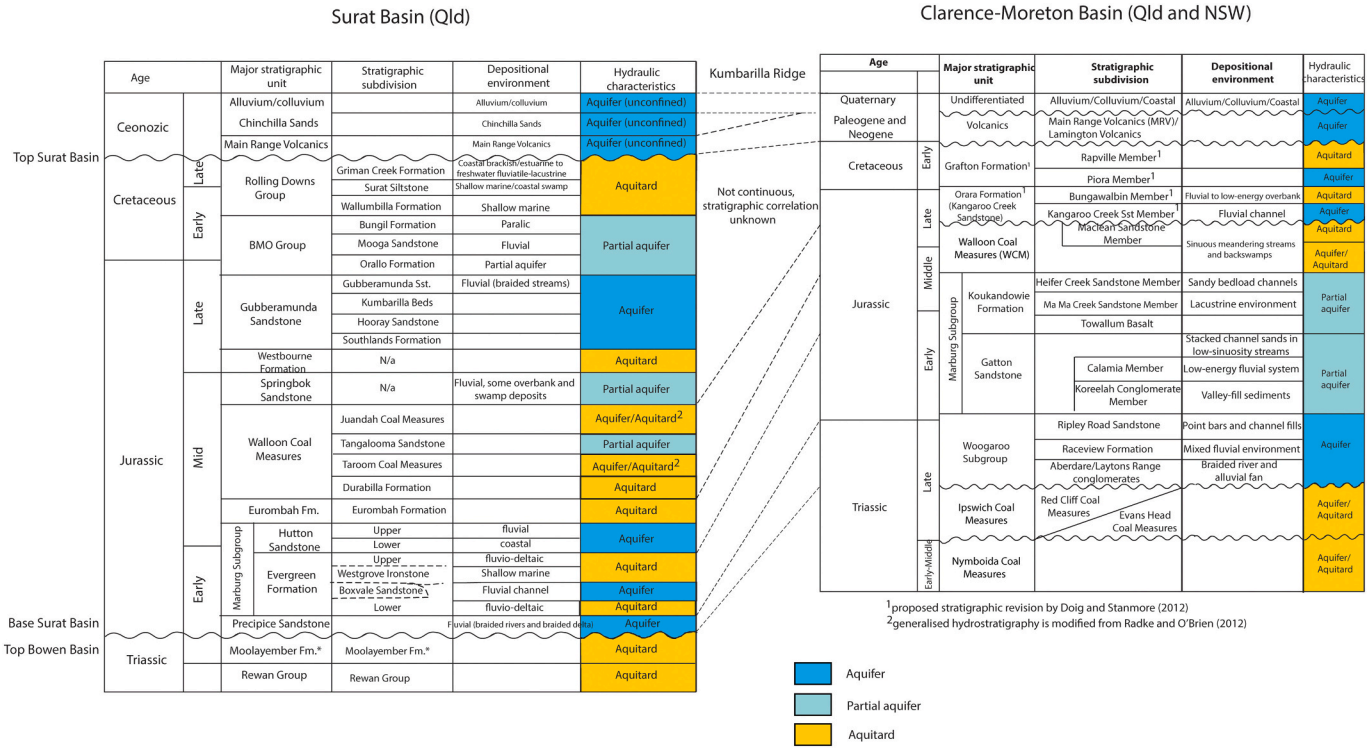

Fig. 2. Stratigraphic table of Surat and Clarence-Moreton basins. Based on Exon (1976), O'Brien and Wells (1994), Wells and O'Brien (1994), Green et al. (1997), Doig and Stanmore (2012) and OGIA (2021b).

between aquifers and between groundwater and surface water depends on a reliable assignment of the screened intervals to a particular hydrostratigraphic formation (Raiber and Suckow, 2017).

A key challenge is the availability of bore construction and aquifer information for the sampled bores. Bore construction and reporting standards have evolved over time, and therefore the quality and completeness of bore records held in the Queensland groundwater database (DNRME, 2020) is variable. In some cases, there is incomplete or limited construction information available and inconsistent information about source aquifers (Erasmus et al., 2024). Furthermore, where stratigraphic data exist, these are sometimes incorrect or exist only for part of the bore depth profile. The depth of bores is often unknown, as are the top and/or bottom of the screened interval.

In this study, we used bore casing construction information (e.g. depth of screened interval) (DNRME, 2020) and other geological and hydrogeological data (e.g. geological maps or stratigraphic logs from nearby wells) to assess aquifer membership. In addition, we used existing 3D-geological models developed for the SCM basins (OGIA, 2021b; Raiber et al., 2017) to independently confirm the hydrostratigraphic formation at the screened interval. For this purpose, the screened intervals were imported into the 3D-geological models using Gocad/SKUA software™ (Emerson-Paradigm Geophysical Pty Ltd) for Raiber et al. (2017) and Petrel (Schlumberger) for the Queensland Office of Groundwater Impact Assessment (OGIA, 2021b; Erasmus et al., 2024). The models were then queried to identify the formation where the bores are screened. Close to the basin margin and intake beds of the Hutton Sandstone, Evergreen Formation and Precipice Sandstone in the northern and eastern parts of the Surat Basin (Fig. 1), there are few stratigraphic or exploration wells and only a small number of groundwater bores with reliable bore casing construction detail and stratigraphic data; the uncertainty of bore-aquifer assignments is therefore higher in these areas.

3.2. Sample collection

Groundwater samples included in this analysis were collected from water supply and groundwater monitoring bores and CSG production wells in the SCM basins during multiple projects by collaborating organisations (Appendix A) which are presented collectively here for the first time. In addition, existing Sr isotope results for groundwater samples in the SCM basins were compiled from Baublys et al. (2019), Duvert et al. (2015), Feitz et al. (2014) and Hofmann et al. (2024), resulting in a combined groundwater $^{87}Sr/^{86}Sr$ data set of 452 groundwater samples (Appendix A; with values for 298 groundwater samples presented here for the first time). Data from bores where the aquifer assignment could not be confirmed with high confidence, or which are screened across different formations, were not included in the statistical assessment ($n = 25$).

Groundwater natural radioactive age tracers (^{14}C and ^{36}Cl) and hydrochemical data (Appendix A) are from this study, Baublys et al. (2015), Baublys et al. (2021), Duvert et al. (2015), Feitz et al. (2014), DNRME (2020), Scheiber et al. (2020), Suckow et al. (2016, 2020, 2021), Raiber et al. (2022) and Hofmann et al. (2024). Surface water samples were collected from Lockyer Creek, a major agricultural catchment within the CMB, and 15 of its tributaries during low-flow conditions (mostly during 2011–2013) at 32 locations (Fig. 1; Section 5.3) to determine the usefulness of $^{87}Sr/^{86}Sr$ isotopes for identification of the source aquifer of stream flow during baseflow conditions.

3.3. Analytical procedures and data sources

Strontium isotope compositions in groundwaters (298 new samples) and surface water ($n = 33$) collected from the SCM basins over the period 2011 to 2022 were analyzed at the School of Geography, Earth and Atmospheric Sciences (SGEAS) of the University of Melbourne (Maas et al., 2015), the Department of Earth Sciences at the University of Adelaide and at the CSIRO Radiogenic Isotope Facility (Sydney). The detailed analytical methodologies for $^{87}Sr/^{86}Sr$ analysis are described in Appendix B.

In addition to published groundwater age tracer results, groundwater samples were analyzed for radiocarbon (^{14}C) with a half-life of 5730 years and chloride-36 (^{36}Cl) (half-life of 301,000 years) by accelerator mass spectrometry (AMS) at the Australian Nuclear Science and Technology Organisation (ANSTO), Lucas Heights, and at the Australian National University (ANU). ANSTO measurement of ^{14}C followed the methods described by Fink et al. (2004) while samples for ^{36}Cl followed the methods outlined by Wilcken et al. (2017). Samples analyzed at the Australian National University (ANU) for ^{36}Cl following the methods described by Fifield (1999) and Fifield et al. (2013). Measured data of ^{36}Cl is reported in the given ratio of ^{36}Cl atoms to the total chloride concentration ($^{36}Cl/Cl$).

Major ion data were collated from multiple studies (Baublys et al., 2019; DNRME, 2020; OGIA, 2023; Raiber and Suckow, 2017; this study) to provide context on benefits and limitations of major ion hydrochemical data. Although samples in this and previous studies were collected during many different projects and analyzed for major ion composition at many different laboratories, samples were typically analyzed using standard analytical techniques (e.g. titration and Discrete Analyzer for Alkalinity, Cl and SO_4 and ICP-MS or ICP-AES for cations). Salinity of groundwater and surface water is represented by the electrical conductivity (expressed as μS/cm).

3.4. Core sample collection and whole rock analysis

Existing whole rock $^{87}Sr/^{86}Sr$ data of Cenozoic volcanic ($n = 26$) and Surat Basin rocks ($n = 19$) were collated from Baublys et al. (2019), Ewart et al. (1988), and Horner et al. (2015). Additional whole rock analyses ($n = 39$) were conducted for this study on core samples from SCM basins collected from the Queensland core library (Exploration Data Centre, Zellmere, Qld). The sampling strategy was to achieve a balance between characterizing the entire or majority of the vertical sequence of hydrostratigraphic formations at two sites (Chinchilla 4 and Roma 8 stratigraphic wells) whilst at the same time obtaining a good representation of spatial variability for the major aquifers. This includes the first $^{87}Sr/^{86}Sr$ core analyses from the Clarence-Moreton Basin (Fig. 1). All rock samples are shown in Appendix C.

The $^{87}Sr/^{86}Sr$ of whole-rock samples ($n = 37$) were analyzed at the School of Geography, Earth and Atmospheric Sciences (SGEAS) of the University of Melbourne. In addition, leachates of two rocks samples (Precipice and Hutton sandstones) following treatment (partial digestion) with a weaker acid (1 M acetic acid) were also analyzed at the University of Melbourne as a comparison with the whole rock $^{87}Sr/^{86}Sr$. Rock samples ($n = 24$) for Mid Jurassic rocks (Walloon Coal Measures and Springbok Sandstone) subjected to sequential leaching with ammonium acetate and acetic acid were also compiled from Baublys et al. (2019).

4. Results

4.1. Groundwater hydrochemistry

In sedimentary basins, groundwater hydrochemical evolution along its flow path is influenced by many hydrogeochemical processes, such as water–rock interactions as well as inter–aquifer mixing across leaky aquitards or along major fault lines (Mallants et al., 2016). Determining source aquifers for surface water or springs, study aquifer connectivity or confirm aquifer membership can be challenging, particularly if relying solely on the use of traditional major ion chemistry and multiple lines of hydrogeological evidence are often necessary to substantiate conclusions (Flook et al., 2020).

To illustrate this challenge for the SCM basins, we present a series of diagrams (Fig. 3) showing major ion chemistry within the Main Range

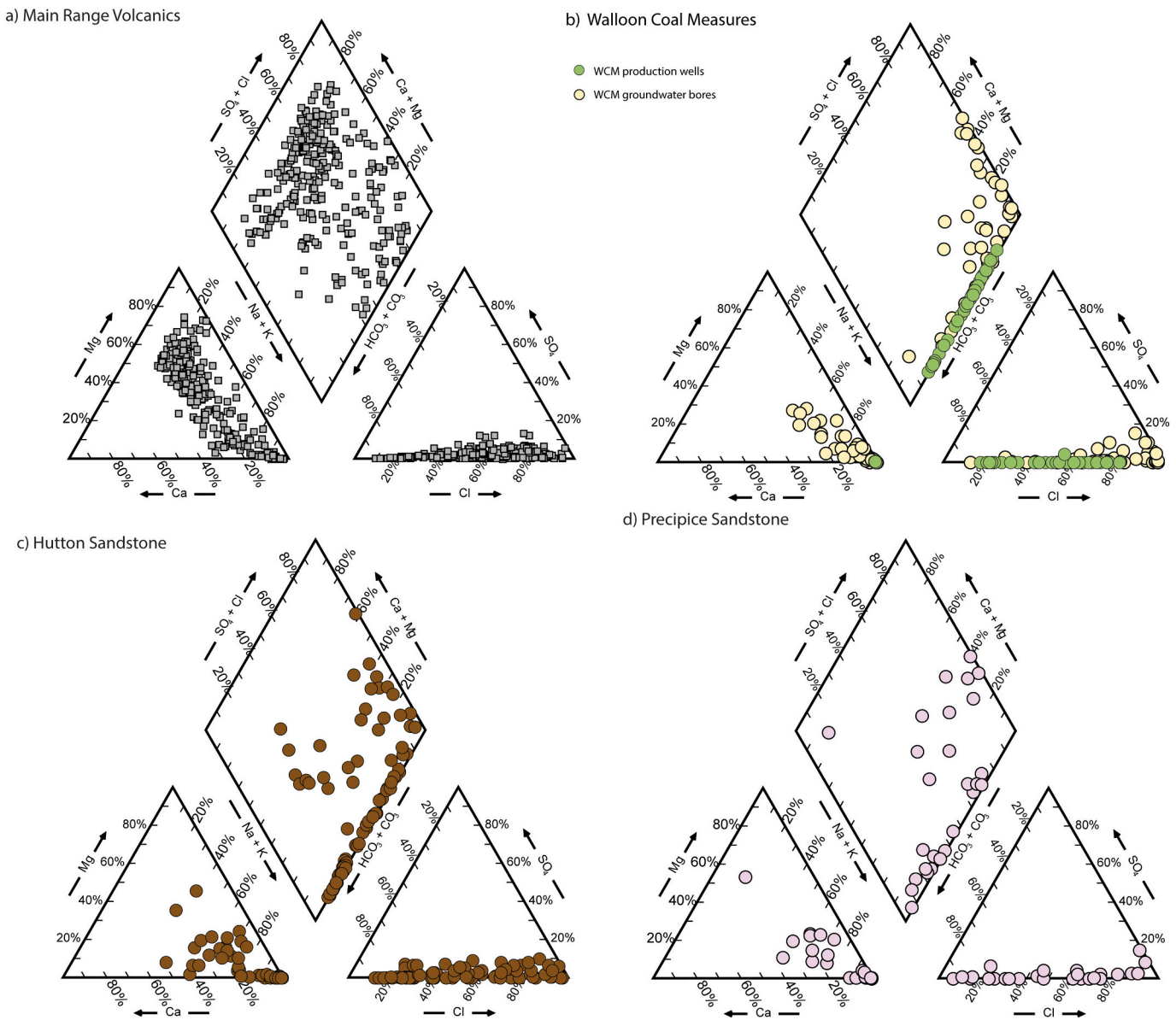

Fig. 3. Piper plot showing hydrochemistry of a) Main Range Volcanics, b) Walloon Coal Measures (WCM), c) Hutton Sandstone, and d) Precipice Sandstone within the Surat and Clarence-Moreton basins. Data are compiled from Baublys et al., 2019 (WCM production wells); DNRME, 2020; OGIA, 2023; Raiber and Suckow, 2017.

Volcanics, Walloon Coal Measures (CSG target strata), and two of the key aquifers (Hutton Sandstone and Precipice Sandstone). This high-level regional assessment shows multiple patterns. For example, when comparing the hydrochemistry of the Main Range Volcanics and the Walloon Coal Measures (Fig. 3a and b), there are some distinct differences: Ca- and Mg-rich groundwaters (Ca-Mg-HCO_3 water types) commonly found in the Main Range Volcanics are entirely absent within the Walloon Coal Measures. On the other hand, groundwater samples depleted in sulfate (SO_4), Ca and Mg are almost absent within the Main Range Volcanics, whereas they are very common in most Walloon Coal Measures groundwater samples (especially for CSG-production waters) (Fig. 3a and b). In contrast, as suggested by Raiber and Suckow (2017), there are some similarities in major ion chemistry between the adjacent Walloon Coal Measures and Hutton Sandstone in the northern Surat Basin. This can be observed in Fig. 3b and c, where groundwaters with very low Ca, Mg and SO_4 concentrations are common occurrences in both formations, and where both HCO_3- and Cl-dominated water types exist in both formations. Likewise, there are overlaps between the major ion chemistry of the Hutton Sandstone and Precipice Sandstone in some areas (Fig. 3c and d).

4.2. Strontium isotope ratios ($^{87}Sr/^{86}Sr$)

In the following sections, the median value is used as the primary statistical parameter for comparison of $^{87}Sr/^{86}Sr$ sample population characteristics in different formations as this measure of central tendency is less sensitive to extreme values than the mean (Helsel and Hirsch, 2002). Detailed summary statistics (minimum, maximum, mean, median and skewness) for water and whole-rock $^{87}Sr/^{86}Sr$ in each formation were derived using StatGraphics Centurion statistical software (Manugistics Inc., USA) (Appendix B); the summary statistics are provided in Table 1.

4.2.1. Strontium whole rock ratios

Aquifer whole rock $^{87}Sr/^{86}Sr$ of key formations within the SCM basins were compiled from the literature (Section 3.4) and complemented with rock samples collected and analyzed during this study. Sampling locations are shown in Fig. 1, and the vertical profiles of $^{87}Sr/^{86}Sr$ in two

Table 1
Summary statistics of whole rock and groundwater $^{87}Sr/^{86}Sr$ of major aquifers in the Surat and Clarence-Moreton basins. For more information on the statistical assessment, see Appendix B.

	Number	Minimum	Maximum	Average	Median	Standardised skewness
Groundwater and surface water $^{87}Sr/^{86}Sr$						
Surface water (creeks and springs)	40	0.70355	0.70912	0.70526	0.70498	2.79
Alluvium	79	0.70385	0.70779	0.70495	0.70491	5.25
Main Range Volcanics and equivalents[a]	12	0.70355	0.70548	0.70425	0.70422	1.01
Bungil, Mooga and Orallo Fm. (BMO)	9	0.70431	0.70480	0.70443	0.70443	2.32
Gubberamunda Sandstone (and Hooray Sandstone)	16	0.70437	0.70703	0.70546	0.70519	1.14
Springbok Sandstone	19	0.70367	0.70712	0.70481	0.70470	1.52
Walloon Coal Measures all	104	0.70324	0.70583	0.70379	0.70364	7.23
Walloon Coal Measures groundwater bores	59	0.70324	0.70583	0.70396	0.70380	3.86
Walloon Coal Measures production wells	45	0.70328	0.70449	0.70359	0.70351	4.25
Hutton Sandstone (Koukandowie Formation)	119	0.70340	0.70755	0.70515	0.70511	3.16
Evergreen Formation (Gatton Sandstone)	13	0.70503	0.70830	0.70631	0.70629	1.15
Marburg Subgroup undifferentiated	4	0.70585	0.70813	0.70705	0.70711	N/A
Precipice Sandstone (Woogaroo Subgroup)[b]	52	0.70559	0.70932	0.70710	0.70698	3.36
Early Jurassic formations (Precipice Sandstone, Evergreen Formation and Hutton Sandstone)	188	0.70339	0.70932	0.70584	0.70566	3.52
Mid Jurassic to Cretaceous formations (Walloon Coal Measures, Springbok Sandstone, Gubberamunda Sandstone and BMO)	139	0.70324	0.70712	0.70413	0.70388	7.09
Unknown/highly uncertain aquifer, inter-aquifer	24	0.70377	0.70705	0.70511	0.70496	1.30
Westbourne Formation	1	0.70400	0.70400	N/A	N/A	N/A
Total number of individual water samples[c]	484					
Rock $^{87}Sr/^{86}Sr$						
Cenozoic volcanics	23	0.70313	0.70467	0.70384	0.70374	1.29
Orallo Formation	1	0.70567	0.70567	N/A	N/A	N/A
Gubberamunda Sandstone	2	0.70552	0.70852	N/A	N/A	N/A
Westbourne Formation	2	0.70416	0.70516	N/A	N/A	N/A
Springbok Sandstone (whole rock)	2	0.70400	0.70417	N/A	N/A	N/A
Springbok Sandstone (partial digestion)	2	0.70374	0.70378	N/A	N/A	N/A
Walloon Coal Measures (whole rock)	14	0.70358	0.70829	0.70513	0.70446	1.58
Walloon Coal Measures (partial digestion ammonium acetate, acetic acid)	24	0.70330	0.70461	0.70380	0.70371	1.57
Hutton Sandstone (Koukandowie Formation) whole rock	12	0.71047	0.72555	0.71892	0.71892	−0.48
Evergreen Formation (Gatton Sandstone)	10	0.70853	0.71125	0.70983	0.70985	−0.09
Precipice Sandstone (Woogaroo Subgroup) whole rock	9	0.71069	0.72744	0.71830	0.71672	0.43
Early Jurassic formations (Precipice Sandstone, Evergreen Formation and Hutton Sandstone) (whole rock)	31	0.70853	0.72744	0.71581	0.71636	1.12
Mid Jurassic to Cretaceous formations (Walloon Coal Measures, Springbok Sandstone, Gubberamunda Sandstone and BMO) (whole rock)	25	0.70358	0.70852	0.70519	0.70424	2.05
Total number of individual rock samples	101					

[a] Three springs within the headwaters of the Main Range Volcanics are included.
[b] Five springs within the Precipice Sandstone are included.
[c] Samples of springs in MRV and Precipice Sandstone are included in "Total number of individual water samples" once as part of aquifer categories.

representative petroleum and stratigraphic wells (Chinchilla 4 and Roma 8) are shown in Fig. 4. The whole rock $^{87}Sr/^{86}Sr$ of important aquifers within the SCM basins is shown in Fig. 5a (only data for formations with >5 measurements are shown). All whole rock data are presented in Appendix C and summary statistics are shown in Table 1.

The vertical profiles of $^{87}Sr/^{86}Sr$ at Chinchilla 4 (25 whole rock samples analyzed throughout the entire stratigraphic sequence) and Roma 8 (11 samples collected from the Early Jurassic formations within the Surat Basin) shows that although some within-formation variability exists, there are distinct patterns of separation between adjacent formations (Fig. 4). Within the Early Jurassic strata, the whole rock $^{87}Sr/^{86}Sr$ of the Precipice Sandstone ($n = 9$, median of 0.71672 and standardised skewness of 0.43) and the Hutton Sandstone ($n = 12$, median of 0.71892 and standardised skewness of −0.48) are similar but distinct from the intervening Evergreen Formation ($n = 10$, median of 0.70985 and standardised skewness of −0.09) throughout the SCM basins (Fig. 5). Two rock samples from the Precipice Sandstone and the Hutton Sandstone partially digested with a weaker acid (acetic acid) have significantly lower $^{87}Sr/^{86}Sr$ than the corresponding whole rock ratios (0.70757 and 0.70766 compared to 0.71294 and 0.72514, respectively).

The whole rock $^{87}Sr/^{86}Sr$ of the Hutton Sandstone differs significantly from that of the overlying Walloon Coal Measures ($n = 14$, median of 0.70446 and a standardised skewness of 1.58). Based on a smaller number of analyses, the whole rock $^{87}Sr/^{86}Sr$ of the younger formations within the Surat Basin (Late Jurassic to Cretaceous, which are not present in the Queensland part of the Clarence-Moreton Basin) appear to be slightly more radiogenic (higher $^{87}Sr/^{86}Sr$) than most of the Walloon Coal Measures samples in the Chinchilla 4 depth profile (not shown in Fig. 5a but in the depth profile of Fig. 4). The exception to this is the Taroom Sandstone (a sandstone within the Taroom Coal Measures member of the Walloon Coal Measures; Figs. 2, 4), which has higher $^{87}Sr/^{86}Sr$ than the overlying Late Jurassic to Cretaceous formations but is also significantly less radiogenic than the underlying older hydrostratigraphic formations within the SCM basins. Walloon Coal Measures samples subjected to treatment with ammonium acetate or acetic acid have a lower median $^{87}Sr/^{86}Sr$ ($n = 24$; 0.70371). However, none of the samples with elevated $^{87}Sr/^{86}Sr$ were subjected to sequential leaching.

Insufficient core samples were analyzed for a statistical assessment of $^{87}Sr/^{86}Sr$ within the Mid-Jurassic to Cretaceous strata (BMO Group, Gubberamunda Sandstone, Westbourne Formation and Springbok Sandstone). However, the available data indicate that these ratios are generally less radiogenic (ranging from 0.70400 to 0.705667), except for one sample from the Gubberamunda Sandstone, which has a higher $^{87}Sr/^{86}Sr$ of 0.708515 (Appendix C).

The comparison of whole rock $^{87}Sr/^{86}Sr$ in Early Jurassic and Mid Jurassic (Precipice Sandstone, Evergreen Formation and Hutton Sandstone) to Cretaceous Formations (Walloon Coal Measures, Springbok

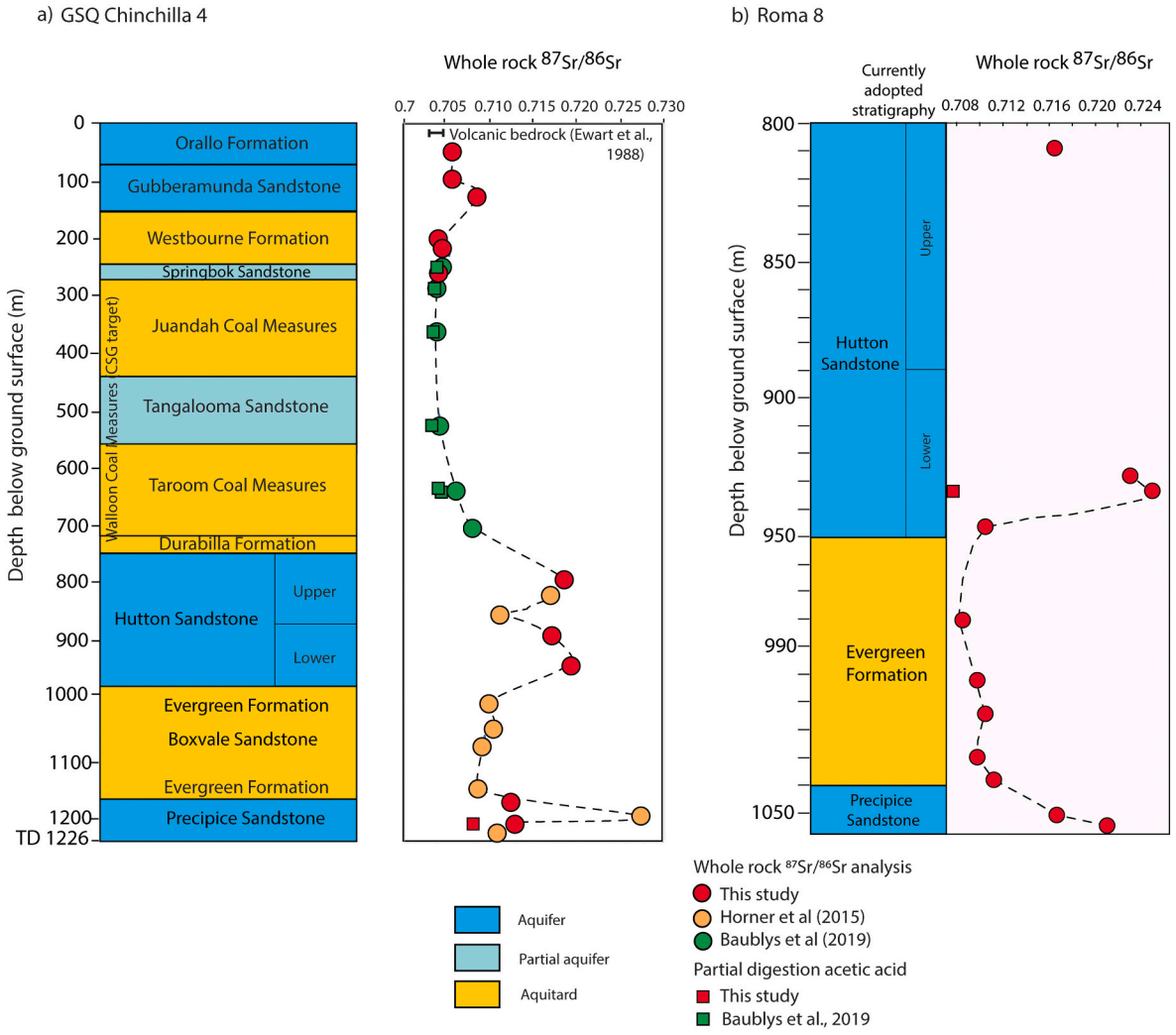

Fig. 4. Vertical profiles of whole-rock and partially digested whole rock $^{87}Sr/^{86}Sr$ (collected and compiled during this study) at Roma 8 and Chinchilla 4 stratigraphic wells. For locations of wells, see Fig. 1.

Sandstone, Gubberamunda Sandstone, BMO Group and Westbourne Formation) shows that the Early Jurassic formations have significantly higher ratios (median of 0.71636 compared to 0.70424; Table 1).

Although not present within Chinchilla 4 and Roma 8 stratigraphic wells, the Main Range Volcanics and chronological equivalent Cenozoic volcanic rocks form a very significant aquifer in some parts of the SCM basins. Based on data from Ewart et al. (1988), the Main Range Volcanics and equivalents within or close to the SCM basins have the lowest $^{87}Sr/^{86}Sr$ of all formations assessed within this study ($n = 26$, median of 0.70375, standardised skewness of 0.25). Furthermore, the variability of $^{87}Sr/^{86}Sr$ within the Main Range Volcanics and equivalents is minor (Fig. 5a).

4.2.2. Rainfall

Previous studies elsewhere in Australia (e.g. in Victoria; Raiber et al., 2009) confirmed that $^{87}Sr/^{86}Sr$ of rainfall varied with distance from the coast due to the incorporation of atmospheric dust. Two rainfall samples analyzed for the current study (Fig. 1) yielded $^{87}Sr/^{86}Sr$ of 0.707688 and 0.709141. Previously reported rainfall $^{87}Sr/^{86}Sr$ in Dalby (Hofmann et al., 2024) and Chinchilla (Baublys et al., 2019) (Fig. 1) of 0.70640 and 0.70822 were also within a similar range. The rainfall samples with the lower $^{87}Sr/^{86}Sr$ are less radiogenic than modern seawater (~0.709; Veizer, 1989), which represents the starting point of meteoric water. This may indicate the incorporation of windblown dust into rainfall or subsequently into the rainfall sampler (i.e. dust originating from local basalt soils, which prevail in the eastern part of the Surat and western part of the Clarence-Moreton basins).

4.2.3. Groundwater and surface water

The $^{87}Sr/^{86}Sr$ of groundwaters in the SCM basins range from 0.70324 to 0.70932 (Table 1 and Fig. 5), with a median of 0.704697. Strontium concentrations range from 0.001 mg/L to 50.2 mg/L, with a median of 0.72 mg/L. The variability and evolution of $^{87}Sr/^{86}Sr$ within different formations along the flow paths, as well as inter-formational differences, was further assessed using comparisons of $^{87}Sr/^{86}Sr$ with multiple parameters (e.g. salinity (Fig. 6), bore depth (Fig. 7), and groundwater age tracers represented by ^{14}C and ^{36}Cl (Fig. 8)).

4.2.3.1. Precipice Sandstone (and CMB equivalent Woogaroo Subgroup).

Groundwater in the Precipice Sandstone/Woogaroo Subgroup has a minimum $^{87}Sr/^{86}Sr$ of 0.705592 and a maximum ratio of 0.709317 ($n = 52$, including 5 spring samples), median of 0.70698; standardised skewness of 3.36 (Table 1). Although most groundwater samples collected from the Precipice Sandstone are fresh, some samples have higher salinity, which has been attributed to possible fault-induced connection with underlying formations (Raiber and Suckow, 2017; Raiber et al., 2022).

Groundwater samples within or close to the intake beds of the

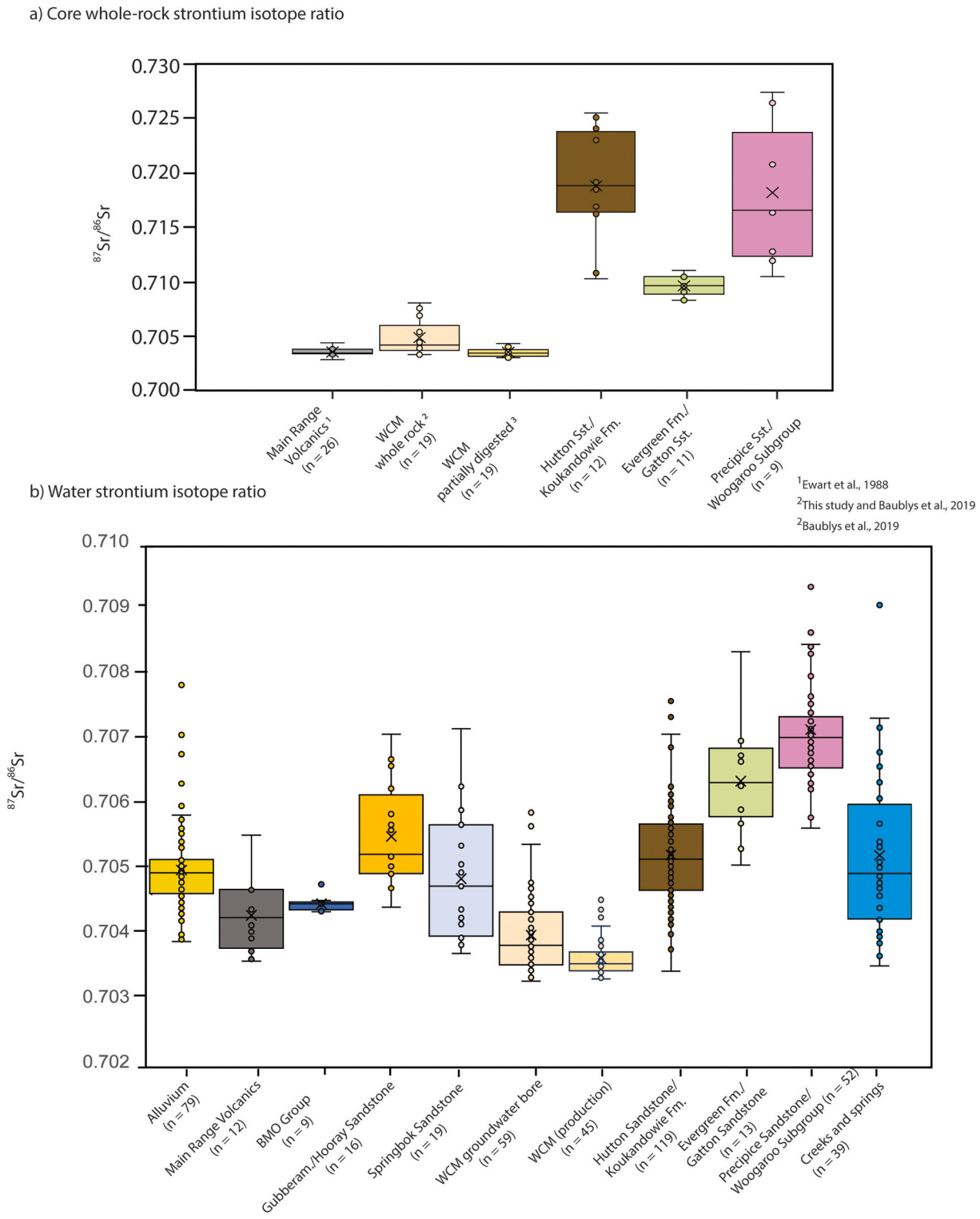

Fig. 5. a) Strontium isotope ratios of whole-rock core samples, and b) water (groundwater and surface water) $^{87}Sr/^{86}Sr$ ratios in the Surat and Clarence-Moreton basins. Points above the whiskers represent outliers. For more information, see Appendix B. WCM corresponds to the Walloon Coal Measures. BMO Group corresponds to the Bungil Formation, Mooga Sandstone and Orallo Formation.

Precipice Sandstone at the basin margin have comparatively high ^{14}C (up to about 61 % Modern Carbon (pMC)). Radiocarbon contents above quantification limit have been detected in most samples (Appendix A), despite the considerable depth from which the samples were collected (>1000 m below ground surface for some samples). As discussed by OGIA (2016), Crosbie et al. (2022), Raiber et al. (2022), and Suckow et al. (2018, 2020), recharge rates to the Precipice Sandstone are high (mean recharge of approximately 11 mm/year in Precipice Sandstone in the northern Surat Basin), reflecting the predominantly coarse grain-size composition with only limited cementation. The comparison of $^{87}Sr/^{86}Sr$ with ^{14}C (Fig. 8) shows that there is no change in $^{87}Sr/^{86}Sr$ with decreasing radiocarbon activity (longer contact time with the aquifer) for the Precipice Sandstone.

The highest and lowest $^{36}Cl/Cl$ values measured in the Precipice

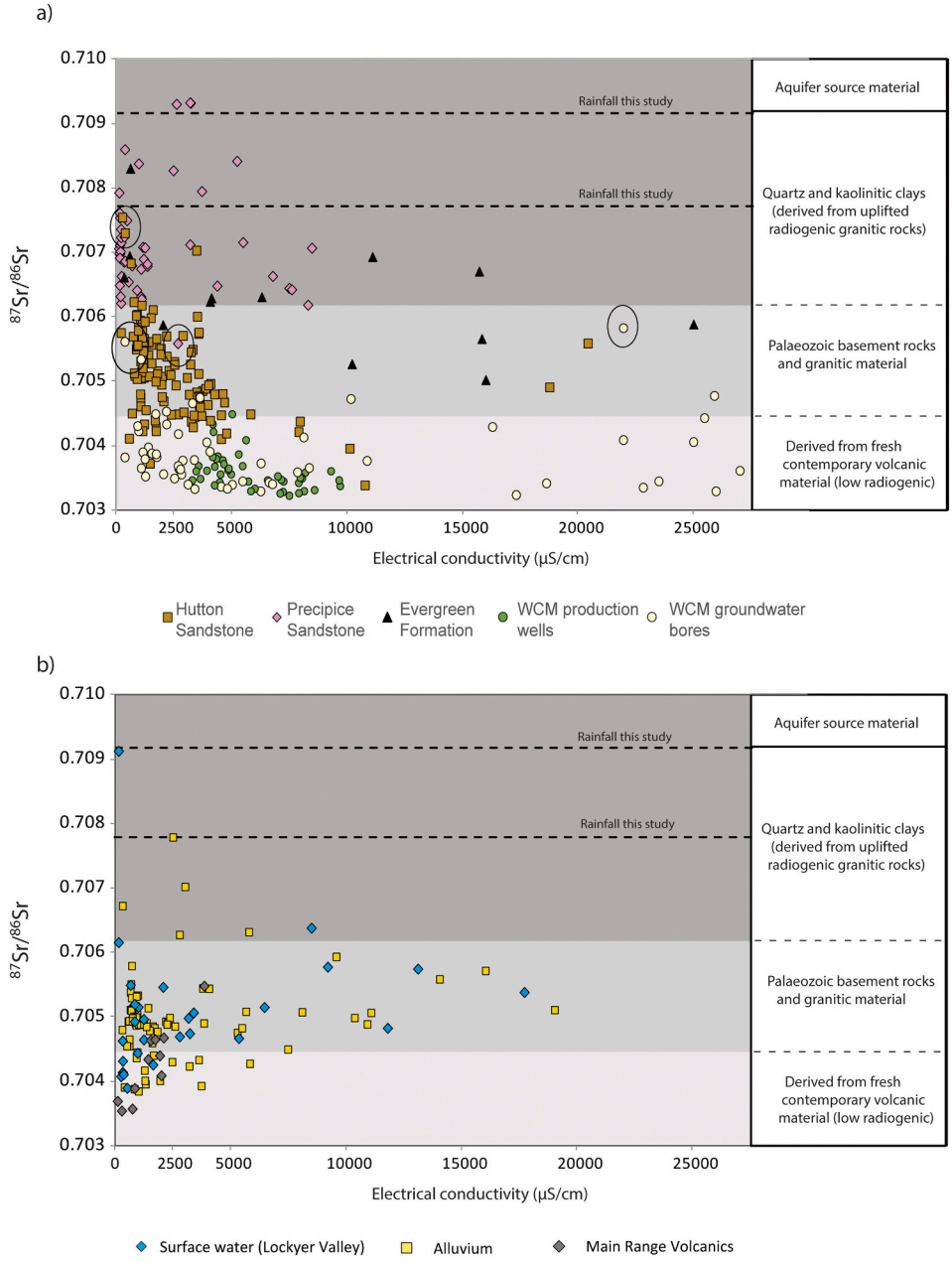

Fig. 6. a) $^{87}Sr/^{86}Sr$ isotope ratios versus salinity (represented by the electrical conductivity) of groundwater samples in major aquifers within the Surat and Clarence-Moreton basins and b) in surface water (creeks and springs) and alluvial and Main Range Volcanics groundwater samples.

Sandstone are ~190 × 10^{-15} and 4 × 10^{-15}. As suggested by Suckow et al. (2018), underground production resulted in an equilibrium of approximately 10 × 10^{-15} in Hutton Sandstone groundwater, with similar or only slightly lower values (above 6 × 10^{-15}) expected for the Precipice Sandstone. This indicates that the lower values represent the practical limit for $^{36}Cl/Cl$ in the Precipice Sandstone. As for ^{14}C, there are no changes in $^{87}Sr/^{86}Sr$ with increasing groundwater residence time represented by the longer time scales of ^{36}Cl.

4.2.3.2. Hutton Sandstone (and CMB equivalent Koukandowie Formation). The $^{87}Sr/^{86}Sr$ of the Hutton Sandstone/Koukandowie Formation groundwater is typically lower than that of the Precipice Sandstone and within a narrower range of between 0.703394 and 0.707548 (n = 119, median of 0.705113, standardised skewness of 3.16) (Table 1 and; Fig. 5).

Similar to the Precipice Sandstone, the comparison of $^{87}Sr/^{86}Sr$ in groundwater and the mid-screen depth within the Hutton Sandstone does not show any significant changes from the shallow margins to the deeper part of the basins (Fig. 7b and c). Likewise, a comparison of the evolution of $^{87}Sr/^{86}Sr$ along selected inferred flow paths within the Hutton Sandstone does not reveal any distinct patterns. Along one flow path in the Northern Surat Basin, the $^{87}Sr/^{86}Sr$ in groundwater closest to the recharge area is elevated, and rapidly decreases with distance from the basin margin. However, flow path delineation and bore-aquifer attribution near the intake beds of the Hutton Sandstone in the northern Surat Basin are highly uncertain due to a high degree of geological complexity and a lack of reliable stratigraphic data (Raiber and Suckow, 2017; Raiber et al., 2022). Along two flow paths in the eastern part of the Surat Basin where considerably more stratigraphic and hydraulic data are available, $^{87}Sr/^{86}Sr$ in groundwater does not show such an evolution with increasing distance from the basin margin.

For the Hutton Sandstone, ^{14}C ranges from 0.05 to 65.93 pMC (Fig. 8,

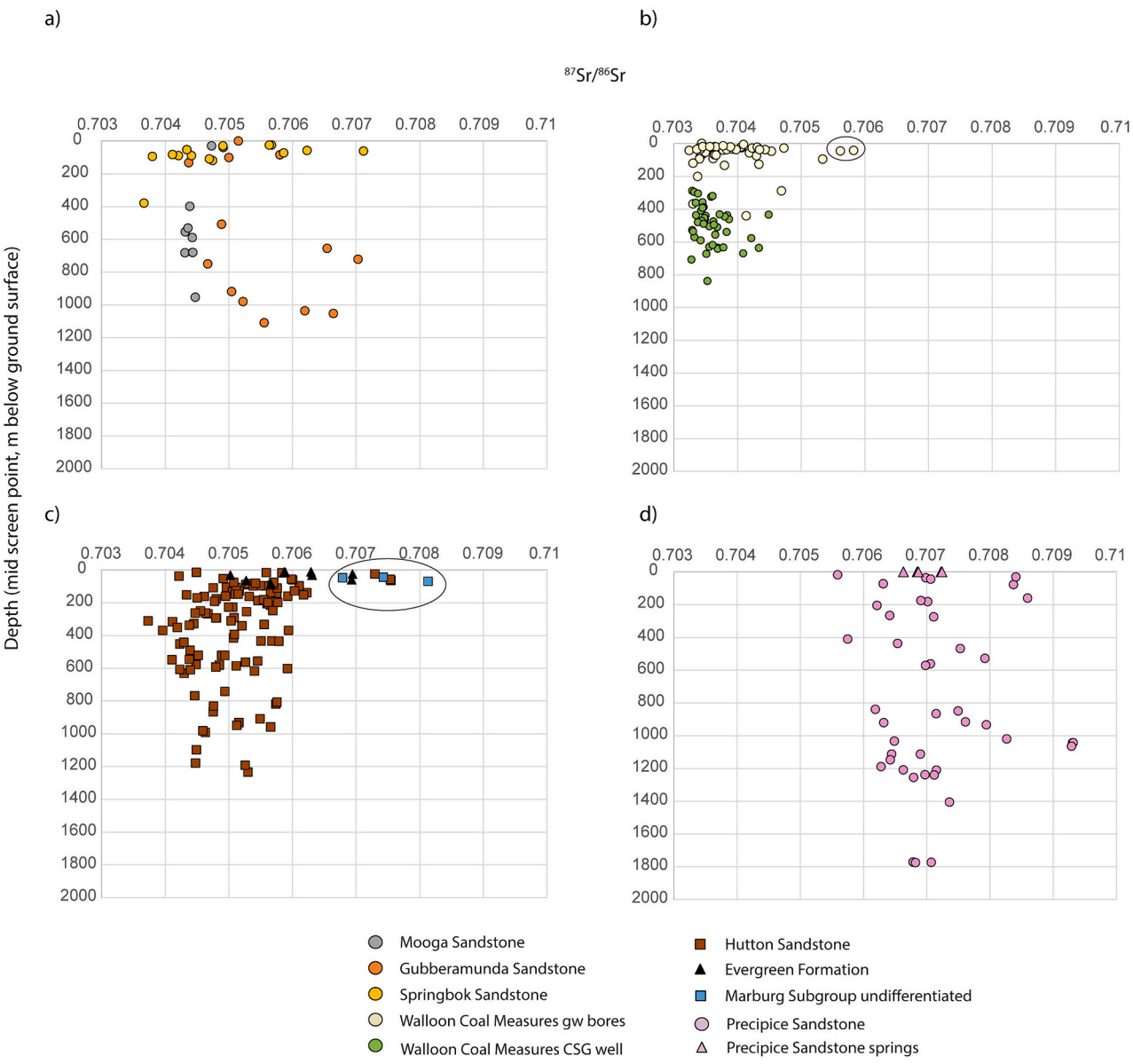

Fig. 7. Strontium isotope ratios ($^{87}Sr/^{86}Sr$) versus bore depth (represented by mid-screen point) for major hydrostratigraphic formations in the Surat and Clarence-Moreton basins. Outliers within the Hutton Sandstone and Walloon Coal Measures and samples within the Marburg Subgroup (including both Hutton Sandstone and Evergreen Formation) are highlighted by black circles.

Appendix A). This includes samples collected from within or close to the outcrop beds of the Hutton Sandstone and samples from the deeper parts of the SCM basins. The comparison of ^{14}C and $^{36}Cl/Cl$ with $^{87}Sr/^{86}Sr$ for groundwater in the Hutton Sandstone shows a moderate correlation (R^2 = 0.35 and 0.34, respectively) (Fig. 8b).

4.2.3.3. Evergreen Formation (and CMB equivalent Gatton Sandstone). The Evergreen Formation and its CMB equivalent Gatton Sandstone, stratigraphically located between the Precipice and Hutton sandstones, has groundwater $^{87}Sr/^{86}Sr$ intermediate between those of the Precipice Sandstone and Hutton Sandstone, ranging from 0.705026 to 0.708299 (n = 13, median of 0.706291; standardised skewness of 1.15) (Table 1 and Fig. 5b). As the Evergreen Formation is not an aquifer at the basin scale in the SCM basins, there are relatively few groundwater bores within this unit and thus only relatively few samples available for this study, with most of these collected from the Clarence-Moreton Basin. As for the Precipice and Hutton sandstones, the comparison of groundwater $^{87}Sr/^{86}Sr$ versus salinity, hydrochemical parameters and Sr concentrations shows no distinct patterns, indicating that the $^{87}Sr/^{86}Sr$ is likely to be independent of groundwater type within the Evergreen Formation.

4.2.3.4. Walloon Coal Measures. The $^{87}Sr/^{86}Sr$ in groundwater bores in the Walloon Coal Measures (mostly from within 100 m of the ground surface; Fig. 7a; Appendix A) range from 0.703244 to 0.705828 (n = 59, median of 0.703799, standardised skewness of 3.86) (Table 1 and Fig. 5b). For coal seam gas production wells in the Walloon Coal Measures (mostly with depths between 300 and 800 m below ground surface (Fig. 7)), $^{87}Sr/^{86}Sr$ ranges from 0.703277 to 0.70449 (n = 45, median of 0.70351, standardised skewness of 4.25). This shows that overall, the range of values in the Walloon Coal Measures groundwater bores is slightly higher than in Walloon Coal Measures gas production wells (Table 1).

The assessment of $^{87}Sr/^{87}Sr$ of Walloon Coal Measures groundwater along selected inferred flow paths did not show any decrease of the strontium isotope ratio along these flow paths. Likewise, the comparison

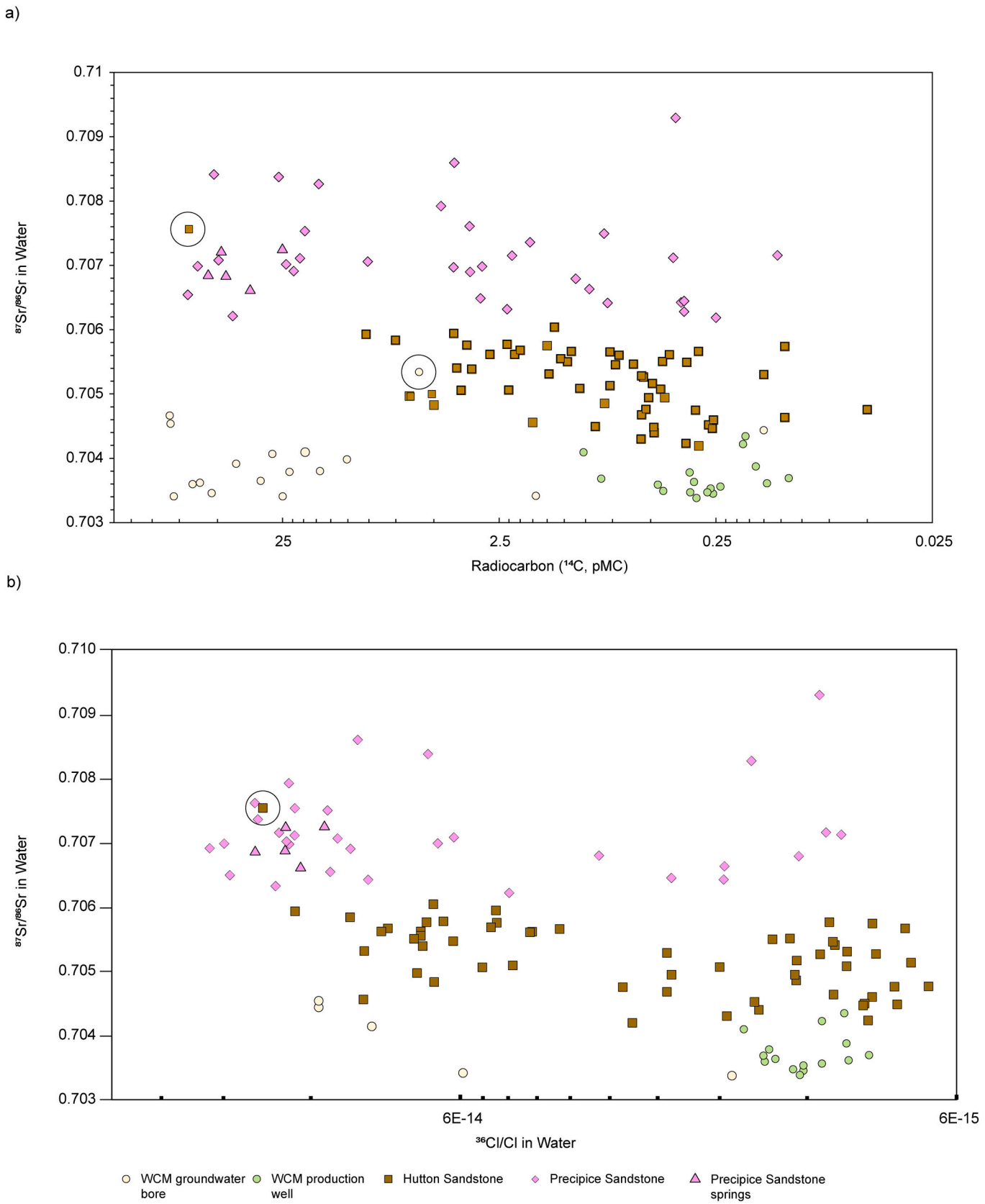

Fig. 8. Strontium isotope ratio ($^{87}Sr/^{86}Sr$) versus a) ^{14}C and b) ^{36}Cl for the Precipice Sandstone, Hutton Sandstone, and Walloon Coal Measures (WCM). Outliers within the Hutton Sandstone and Walloon Coal Measures (WCM) are highlighted by black circles.

with salinity confirms that there are no systematic changes in the Sr isotope ratio with increasing salinity (with salinities ranging from <1000 μS/cm to ~27,000 μS/cm; Fig. 6). Radiocarbon of Walloon Coal Measures groundwaters in the SCM basins ranges from 0.12 to 83 pMC (Fig. 8a). The comparison of $^{87}Sr/^{86}Sr$ and ^{14}C indicates that there is no correlation ($R^2 = 0.0088$) (Fig. 8a). Likewise, $^{36}Cl/Cl$ (Fig. 8b) does not show evidence for a change of $^{87}Sr/^{86}Sr$ with decreasing $^{36}Cl/Cl$, although only relatively few shallow (<100 m) samples from Walloon Coal Measures groundwater bores (n = 4) with $^{36}Cl/Cl$ were available in this study. Determining if one distinct outlier (black circle, Fig. 8a) with an $^{87}Sr/^{86}Sr$ of approximately 0.705340 and a pMC of 5.85 is influenced by connectivity, within-formation lithological variability within the Walloon Coal Measures or other reasons requires a more site-specific assessment.

4.2.3.5. Mid-Late-Jurassic to Cretaceous hydrostratigraphic formations (Springbok, Gubberamunda and Mooga sandstones). The major Mid-Jurassic to Cretaceous hydrostratigraphic formations have lower $^{87}Sr/^{86}Sr$ in groundwater (median of 0.703882) than Early Jurassic formations (median of 0.705661) (Table 1).

The Springbok Sandstone, another important hydrostratigraphic formation which directly overlies the Walloon Coal Measures in the Surat Basin (Fig. 2), has a relatively wide range of $^{87}Sr/^{86}Sr$ in groundwater (n = 19, ranging from 0.703670 to 0.707117, median of 0.704697, standardised skewness of 1.52). Although there are some overlaps with the Walloon Coal Measures, overall, the $^{87}Sr/^{86}Sr$ in groundwater of the Springbok Sandstone and the Walloon Coal Measures (particularly from CSG-production bores) are distinct from each other (Fig. 5b).

The Late Jurassic Gubberamunda Sandstone and BMO Group (where most samples were collected from the Early Cretaceous Mooga Sandstone), sometimes collectively assigned to the Cadna-Owie Hooray aquifer in the GAB (Raiber et al., 2022; Ransley et al., 2015), have groundwater $^{87}Sr/^{86}Sr$ ratios within a narrow range from 0.704311 to 0.707032 (n = 16 and 9, respectively) (median of 0.705189 and 0.704427).

4.2.3.6. Main Range Volcanics. The $^{87}Sr/^{86}Sr$ of groundwaters within the Cenozoic Main Range Volcanics range from 0.70355 to 0.705483 (n = 12, median of 0.704221, standardised skewness of 1.01) (Table 1). As shown in Section 4.1 (Fig. 3), there are some overlaps in hydrochemistry between the Main Range Volcanics and Walloon Coal Measures; however, overall, there are also relatively clear differences between the $^{87}Sr/^{86}Sr$ of groundwater in these formations (Fig. 5b). In contrast, the whole rock $^{87}Sr/^{86}Sr$ of the Main Range Volcanics and the Walloon Coal Measures are relatively similar, with a very narrow range of $^{87}Sr/^{86}Sr$ isotope ratios (Fig. 3a).

No ^{14}C and ^{36}Cl data are available from the Main Range Volcanics for this study. However, Duvert et al. (2015) show that a spring near the headwaters of the Main Range Volcanics at the Great Dividing Range (Fig. 1) in the CMB has a tritium concentration (tritium units, TU) of 1.30 (corresponding to modern water) and $^{87}Sr/^{86}Sr$ of 0.70355.

4.2.3.7. Alluvium. The $^{87}Sr/^{86}Sr$ of groundwater samples within the alluvial aquifers (Condamine River alluvium, Lockyer Valley alluvium and Teviot Brook alluvium) in the Clarence-Moreton Basin range from 0.703849 to 0.707787, with a median of 0.704906 and a standardised skewness of 5.25 (Table 1, based on 79 samples) (Fig. 5b). In general, the $^{87}Sr/^{86}Sr$ of alluvial groundwater samples within the investigated catchments extend over a similar range as the sedimentary and volcanic bedrock groundwater samples and surface water samples.

4.2.4. Surface water

The $^{87}Sr/^{86}Sr$ of surface water samples (creeks and springs) within the SCM basins (n = 40, with most samples collected from the Lockyer Valley; Figs. 1, 9) range from 0.70355 to 0.709123, with a median of 0.70526 and a standardised skewness of 2.79 (Table 1). The range of surface water Sr isotope ratios is very similar to that of groundwaters within the SCM basins (Fig. 5b) and spatial patterns and their controls are described in Section 5.3.

5. Discussion

5.1. Strontium isotopes as a hydrostratigraphic and chemostratigraphic tool

The $^{87}Sr/^{86}Sr$ in groundwater for some aquifers (especially Early Jurassic aquifers) is lower than its whole rock equivalent, whereas only small differences between groundwater and whole rock $^{87}Sr/^{86}Sr$ are observed for other formations (Table 1 and Fig. 5a and b). The whole rock $^{87}Sr/^{86}Sr$ represent the bulk $^{87}Sr/^{86}Sr$ of all mineral phases in a rock, whereas the $^{87}Sr/^{86}Sr$ of groundwater results from the interaction of groundwater with the more reactive and soluble mineral phases. These differences, when present, can be used as a chemostratigraphic or hydrostratigraphic tool (e.g. Raiber et al., 2009; Williamson et al., 2012).

Differences in $^{87}Sr/^{86}Sr$ of mineral phases within a rock can be evaluated further using sequential extraction techniques (e.g. Phan et al., 2018; Baublys et al., 2019), or, as in this study, by partially digesting selected samples with a weaker acid such as 1 M acetic acid. This assessment for two Hutton and Precipice sandstone samples yielded $^{87}Sr/^{86}Sr$ closer to those of groundwater samples (Fig. 4), which represents the more reactive and soluble mineral phases of the rocks. In contrast, the difference between whole rock and partially digested samples for the Walloon Coal Measures (Baublys et al., 2019) are very small (Table 1 and Fig. 4).

The higher whole rock $^{87}Sr/^{86}Sr$ for Hutton and Precipice sandstones compared to $^{87}Sr/^{86}Sr$ in other formations (Fig. 5a) is due to the different aquifer source material. This includes uplifted granitic rocks for the Hutton and Precipice sandstones with higher radiogenic ^{87}Sr compared to volcanic rocks in the Cenozoic Main Range Volcanics and volcanic components in the Jurassic Walloon Coal Measures, which is composed of volcanolithic material associated with contemporary volcanism at the time of deposition of the strata (Jenkinson, 2018; Cook et al., 2013; Fielding, 1993) and have lower content of radiogenic ^{87}Sr. Newly formed mafic igneous rock units (e.g. basalts and volcanic arcs) have the lowest $^{87}Sr/^{86}Sr$, and the median $^{87}Sr/^{86}Sr$ for the Main Range Volcanics (0.70374; Table 1) is consistent with international studies for those types of rocks (~0.703). In contrast, old felsic igneous rock units have the highest measured $^{87}Sr/^{86}Sr$ (>0.720) (Bataille et al., 2018; Peucker-Ehrenbrink and Fiske, 2019).

For the Main Range Volcanics, the median $^{87}Sr/^{86}Sr$ for the groundwater and whole rock are almost equivalent ($\Delta^{87}Sr/^{86}Sr$ = 0.00047, with $\Delta^{87}Sr/^{86}Sr$ representing the difference between the median of whole rock and groundwater $^{87}Sr/^{86}Sr$) (Table 1 and Fig. 5a and b). A small difference in the $^{87}Sr/^{86}Sr$ of the median whole rock and groundwater is observed for the Walloon Coal Measures ($\Delta^{87}Sr/^{86}Sr$ = 0.00082), attributed to Sr cation exchange with montmorillonite and weathering of plagioclase (Baublys et al., 2019). The higher $^{87}Sr/^{86}Sr$ for the Taroom Sandstone (a sandstone within the Walloon Coal Measures) was attributed to the presence of muscovite, which is a source of potassium and thus radiogenic Sr (Baublys et al., 2019). In contrast to the Main Range Volcanics and Walloon Coal Measures, substantially higher differences in $^{87}Sr/^{86}Sr$ from whole rock to groundwater are observed for the Evergreen Formation ($\Delta^{87}Sr/^{86}Sr = 0.00355$) and particularly for the Hutton and Precipice sandstones ($\Delta^{87}Sr/^{86}Sr$ = 0.01381 and 0.00974, respectively).

The Hutton and Precipice sandstones have a very different mineralogy (Farquhar et al., 2013), but both have high $\Delta^{87}Sr/^{86}Sr$ (Fig. 5a and b). The Hutton Sandstone has a more heterogeneous and immature mineralogy including detrital micas, feldspars, lithics, kaolinite,

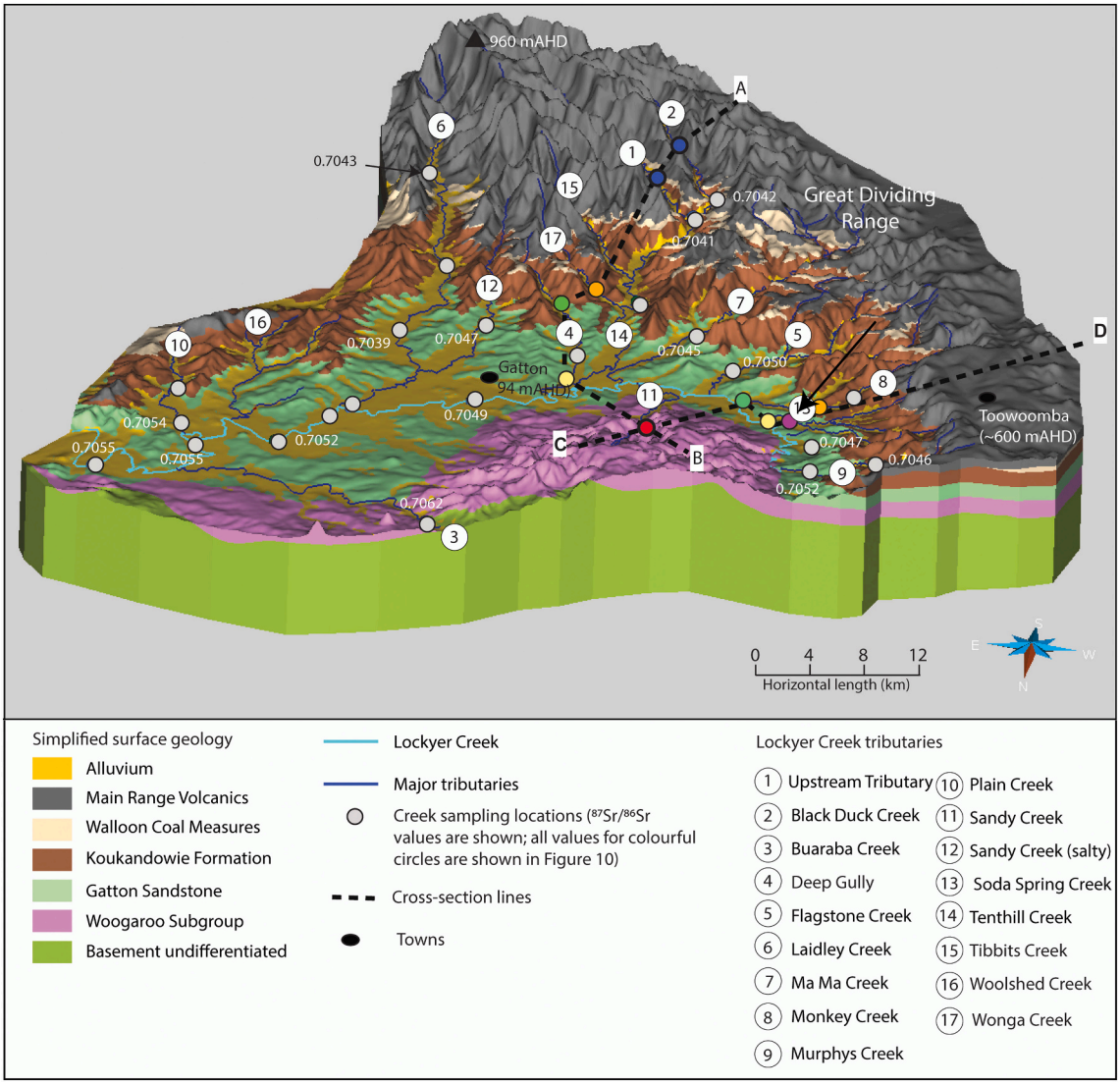

Fig. 9. Surface and spring sampling locations and 3D geological model (developed in GoCAD/SKUA) (Raiber et al., 2019) in the Lockyer Valley. Cross-section orientations and sampling points (colour circles) are shown in Fig. 10. Values for coloured circles are shown in Fig. 10. The elevation mAHD corresponds to metres relative to Australian Height Datum.

smectite, chlorite and Ca–Fe–Mn–Mg carbonates. In contrast, the Precipice Sandstone is chemically mature with high quartz and very low K-feldspar and plagioclase content, but a significant amount of kaolinite clays and minor micas. The kaolinite formed from extensive feldspar and lithic leaching. The maturity of the Evergreen Formation lies between these formations. It appears that the higher permeability and potentially increased weathering of the Hutton and Precipice sandstones, compared to the Evergreen Formation, may be a factor for their much higher $\Delta^{87}Sr/^{86}Sr$.

Weathering of clays rather than feldspars appears to be primarily responsible for controlling the $^{87}Sr/^{86}Sr$ in groundwater for these formations, consistent with CO_2-enhanced weathering of the same formations observed by Horner et al. (2015). Despite the difference in the $^{87}Sr/^{86}Sr$ ratio between the whole rock and groundwater for many of the formations, there remains a significant difference for the $^{87}Sr/^{86}Sr$ in the groundwater between the Walloon Coal Measures and underlying Hutton Sandstone (~0.00147) (Fig. 5b). The groundwater in the Precipice Sandstone also has a significantly higher $^{87}Sr/^{86}Sr$ compared to the Hutton Sandstone (0.00187) (Fig. 3b). The differences in the groundwater $^{87}Sr/^{86}Sr$ provide a practical tool for isotopic fingerprinting of the groundwater source.

The results of the $^{87}Sr/^{86}Sr$ whole rock analysis suggest that Sr isotopes are also useful as a hydrostratigraphic and chemostratigraphic tool. During on-going efforts to further refine the stratigraphy of the Surat Basin, some adjustments of the inter-formation boundaries have been proposed in recent years (e.g. Sobczak et al., 2022; Wang et al., 2019). For example, based on sequence stratigraphy and a lower quartz content in cores of the Precipice Sandstone at Roma 8 than in other locations, Wang et al. (2019) and Hayes et al. (2020) suggested that what was previously described as Precipice Sandstone in stratigraphic well Roma 8 (Fig. 1) is instead the lower part of the Evergreen Formation (Fig. 4); this would indicate that the Precipice Sandstone is absent at this location. However, $^{87}Sr/^{86}Sr$ of this basal part of the stratigraphic sequence is significantly higher than $^{87}Sr/^{86}Sr$ of the Evergreen Formation/Gatton Sandstone (including both mudstone and Boxvale Sandstone intervals) measured in any samples within the SCM basins, and more similar to the Sr isotope ratios of Precipice Sandstone samples in Chinchilla 4 and other wells (Figs. 4 and 5). This suggests that this lower sequence is likely part of the Precipice Sandstone, as originally defined. Additional $^{87}Sr/^{86}Sr$ core analyses from other wells and palynostratigraphy and geochronology from basal Jurassic sequences (complementing the work presented by La Croix et al., 2022) could

provide confirmation of this hypothesis and additional insights into the spatial extent of the Precipice Sandstone.

Furthermore, the surface geology boundaries between hydrostratigraphic formations are still uncertain in some areas, such as in the eastern part of the Surat Basin/western CMB and in the southern Surat Basin in Qld. Here, the boundary between the Hutton Sandstone/Koukandowie Formation and the Evergreen Formation/Gatton Sandstone is not always differentiated in geological maps and they are instead sometimes collectively represented by the Marburg Subgroup (Fig. 2). Despite the relatively high $\Delta^{87}Sr/^{86}Sr$ for the Hutton Sandstone/Koukandowie Formation, there is a characteristic difference in both the whole rock and groundwater $^{87}Sr/^{86}Sr$ of these two members (Hutton Sandstone/Koukandowie Formation and Evergreen Formation/Gatton Sandstone) of the Marburg Subgroup (Fig. 5a and b; Table 1), suggesting that analysis of $^{87}Sr/^{86}Sr$ in rocks and groundwater in the intake beds may also be useful to refine surface geology boundaries in some areas.

5.2. Fingerprinting of aquifers: evolution of strontium isotopes along groundwater flow paths

This study confirms one of the major benefits of Sr isotopes in the SCM basins: $^{87}Sr/^{86}Sr$ ratios are largely independent of hydrochemical variability. For example, the comparison of $^{87}Sr/^{86}Sr$ with parameters such as salinity, bore depth and groundwater residence time (^{14}C and ^{36}Cl) in this study suggests that there is no correlation with these parameters for most formations within the SCM basins, making it an ideal independent tracer to complement hydrochemistry and reduce some ambiguities.

For the SCM basins, the absence of a correlation between $^{87}Sr/^{86}Sr$ and groundwater residence time (Fig. 8) and depth (Fig. 7) within the Precipice Sandstone and the Walloon Coal Measures suggests that the Sr isotope signature of groundwaters in these formations is established early along the flow path within the intake beds (i.e. likely because of water–rock interactions during recharge). A relatively small number of elevated $^{87}Sr/^{86}Sr$ and outliers in the groundwater sample population for example within the Precipice Sandstone and Walloon Coal Measures is responsible for a relatively high skewness and non-normal distribution of the sample population for these formations (Table 1 and Fig. 5).

For the Hutton Sandstone, the moderate statistical relationship observed between ^{14}C and $^{87}Sr/^{86}Sr$ ($R^2 = 0.35$) and $^{87}Sr/^{86}Sr$ and $^{36}Cl/Cl$ ($R^2 = 0.34$) (Fig. 8b) may be due to the dual porosity nature of this formation (Guiton et al., 2015; Suckow et al., 2020), where strontium with a slightly different isotopic composition diffuses from stagnant zones into the more conductive areas. However, the statistical relationship is partially influenced by a single sample with high ^{14}C and ^{36}Cl content which has been identified statistically as an outlier (black circle in Fig. 8a and b). Overall, however, similar to the Precipice Sandstone and the Walloon Coal Measures, $^{87}Sr/^{86}Sr$ for the Hutton Sandstone remains within a narrow range with unique population characteristics. This indicates that an equilibrium between rock and groundwater in these formations is achieved early along a flow path and the likelihood of incorporating new Sr is reduced unless there is a very soluble lithology (e.g. evaporites or carbonates).

There is a wide range of $^{87}Sr/^{86}Sr$ because the alluvium is derived from different sediment sources and the alluvial aquifers interact with different sub-alluvial bedrock formations and surface water in different parts of the catchments. Furthermore, this may also indicate a possible influence of rainfall on the $^{87}Sr/^{86}Sr$ of fresh alluvial groundwaters as indicated in other aquifer system elsewhere (Raiber et al., 2009). The observed range also means that $^{87}Sr/^{86}Sr$ can be used to study connectivity between alluvial and underlying bedrock aquifers and surface waters; however, these local interpretations were outside the scope of the current study.

The results of this study highlight the usefulness of Sr isotopes as an isotopic groundwater fingerprinting tool which can help to increase confidence in the assignments of aquifers to screened intervals and to support the assessment of connectivity between different aquifers. Assigning aquifers screened by monitoring and water supply bores with high confidence and identifying areas of aquifer connectivity/mixing is fundamental to the technical assessments carried out by OGIA. The presence of outliers observed for example for the Precipice Sandstone, Hutton Sandstone and Walloon Coal Measures (Figs. 6a, 7 and 8a and b) likely indicates aquifer interactions/mixing, incorrect bore-aquifer attribution, or local lithological variability within these formations. Although a site-specific assessment of individual outliers is out of scope of this study, further investigations of $^{87}Sr/^{86}Sr$ outliers within the major aquifers and the Walloon Coal Measures (the CSG target) can support groundwater management through identification of data uncertainties and components of the conceptual hydrogeological model that are well understood and highlight areas of major conceptual uncertainty that may require further assessments.

With intensive CSG development areas in the SCM basins (Fig. 1), $^{87}Sr/^{86}Sr$ is now included in routine monitoring obligations to inform ongoing evaluation of connectivity between the CSG target formation and adjacent aquifers (OGIA, 2021a, 2023).

5.3. Comparison with results from previous studies

This finding from the current study contrasts with results and interpretations from previous investigations in the Surat Basin and within the wider GAB. For example, Baublys et al. (2019) suggested that initial recharge waters in the Walloon Coal Measures have higher $^{87}Sr/^{86}Sr$ ratios (~0.705), and that these ratios rapidly decrease from the recharge area to the deeper basin due to a combination of Sr absorption on coal and cation exchange by clays (montmorillonite) (Baublys et al., 2019, 2021). The combination of $^{87}Sr/^{86}Sr$ of groundwater in production wells from Baublys et al. (2019) and our new data from both production wells and groundwater bores (mostly ranging from ~10 m to >100 m depth), including shallow bores within the Walloon Coal Measures outcrop areas in the SCM basins, allows refinement of the findings from Baublys et al. (2019). This combined new dataset shows that the median $^{87}Sr/^{86}Sr$ of the non-production Walloon Coal Measures groundwater bores is only minimally higher than that of the Walloon Coal Measures gas production wells (median of 0.70379 compared to 0.70351) (Fig. 5b), and there are no distinct depth-related $^{87}Sr/^{87}Sr$ patterns within the Walloon Coal Measures (Fig. 7). This suggests that recharge waters quickly equilibrate within the aquifer.

In a previous study which focussed mostly on the Eromanga Basin (the largest sub-basin within the GAB, located west of the Surat Basin), Collerson et al. (1988) suggested that hydrologically young waters exhibit "unradiogenic" (lower) $^{87}Sr/^{86}Sr$, whereas older waters along the flow path are significantly more radiogenic (up to 0.7118). This was attributed by the authors to the possible addition of Sr through dissolution of aquifer silicates. A similar observation was also made by Gwynne et al. (2013) in the south-western GAB. In contrast, no such observations were made during the present study in the SCM basins and in a recent study by Raiber et al. (2022) in the eastern Eromanga Basin, where a characteristic difference in $^{87}Sr/^{86}Sr$ collected from Early and Mid to Late Jurassic aquifers independent of groundwater age was observed. The different observations may for example result from regional differences within the GAB or from the advancement of assignment of bores to individual aquifers in the present study due to the availability of 3D geological models, whereas previous studies have often assigned samples according to classification to broad aquifer sequences (e.g. J and K aquifers, with the "J aquifer" corresponding to the older Jurassic formations and "K aquifer" corresponding to the younger Cretaceous formations).

Low groundwater $^{87}Sr/^{86}Sr$ in sedimentary bedrock aquifers in the eastern Surat Basin was previously attributed to recharge through the Main Range Volcanics (Raiber et al., 2014; Ransley et al., 2015). However, the current study suggests that recharge through Main Range Volcanics has no or only minor regional influence on the evolution of

$^{87}Sr/^{86}Sr$ in groundwater of most sedimentary bedrock aquifers, as there are no discernible differences between $^{87}Sr/^{86}Sr$ in groundwater of sedimentary bedrock aquifers in areas where the Main Range Volcanics are present or absent. Instead, the low $^{87}Sr/^{86}Sr$ of groundwaters in the Mid Jurassic to Cretaceous aquifers likely suggests a volcanolithic source of these sequences.

5.4. Stream source characterization (Lockyer Valley, Clarence-Moreton Basin)

The usefulness of Sr isotopes as a fingerprinting tool is not limited to understanding groundwater. Surface water samples were collected in the Lockyer Valley (Fig. 1) during baseflow conditions to test the usefulness of $^{87}Sr/^{86}Sr$ to determine the source aquifer from reaches overlying the major hydrostratigraphic units (Fig. 9). The comparison of groundwater and surface water $^{87}Sr/^{86}Sr$ shows that they are both within a very similar range (Fig. 5b). Similar to groundwaters in most aquifers, no patterns of distinct changes in surface water $^{87}Sr/^{86}Sr$ with increasing salinity (Fig. 6b) or with water chemistry types were observed in surface waters.

A north–south cross-section based on a 3D-geological model through the Lockyer Valley (Figs. 9, 10, Raiber et al., 2019) from the elevated peaks of the Great Dividing Range in the south (capped by the basalts of the Main Range Volcanics) to the northern outcrop beds of the Woogaroo Subgroup/Precipice Sandstone was used to highlight the spatial patterns of surface water $^{87}Sr/^{86}Sr$ and the influence of bedrock groundwater. In the southern part of the catchment close to the crest of the Great Dividing Range, some of the lowest $^{87}Sr/^{86}Sr$ ratios within the Lockyer Valley were observed in Black Duck Creek and Upstream Tributary (0.7040 and 0.7041, respectively). Based on the $^{87}Sr/^{86}Sr$ of stream water at these sites, the source aquifer could be either the Main Range Volcanics or the Walloon Coal Measures (Fig. 10a). The similarity of both whole rock and groundwater $^{87}Sr/^{86}Sr$ ratios of these two formations (Fig. 5a and b) makes the use of $^{87}Sr/^{86}Sr$ in isolation ambiguous. However, in this instance, the prominence of the Main Range Volcanics with creeks deeply incised into the Main Range Volcanics (Fig. 10a) and the low salinity of surface water in this area (Raiber et al., 2019) suggests that the Main Range Volcanics are the more likely dominant source.

Further downstream, $^{87}Sr/^{86}Sr$ of surface water progressively increases (Figs. 9, 10). At Wonga Creek (incised into the Koukandowie Formation/Hutton Sandstone), the $^{87}Sr/^{86}Sr$ of stream water is outside the range of Main Range Volcanics and Walloon Coal Measures and within the range of the Koukandowie Formation (>0.704). Downgradient of Wonga Creek at Deep Gully (Fig. 10a), $^{87}Sr/^{86}Sr$ is higher than the typical groundwater values of the Koukandowie Formation in this region and within the range of the Gatton Sandstone/Evergreen Formation, into which the stream is incised here. The $^{87}Sr/^{86}Sr$ of Lockyer Creek, the main drainage line within the catchment, is more variable (based on multiple sampling locations); this likely reflects that Lockyer Creek receives a mix of water from multiple tributaries, including tributaries which primarily drain the Main Range Volcanics and smaller tributary systems that mostly drain sedimentary bedrock. Sandy Creek, located further to the north along the cross-section (Fig. 10a and b), is incised into the outcrop beds of the Woogaroo Subgroup/Precipice Sandstone and has the highest $^{87}Sr/^{86}Sr$ (0.709132) of all surface waters within the Lockyer Valley. This reflects the higher $^{87}Sr/^{86}Sr$ of the Woogaroo Subgroup/Precipice Sandstone; due to the freshness and low Sr concentration of this water sample (electrical conductivity of <200 μS/cm), it possibly also indicates some influence of rainwater $^{87}Sr/^{86}Sr$ as demonstrated in other catchments in Australia (Raiber et al., 2009). Towards the lower part of the Lockyer Valley (e.g. Lockyer Creek and Plain Creek; Fig. 9), where there is no influence of the Main Range Volcanics as they are absent or only present as very thin remnants in the headwaters of these creeks (Figs. 9, 10), there is a prevalence of surface water values similar to those of the underlying Koukandowie Formation and Gatton Sandstone.

The observed patterns along these cross-sections and throughout the Lockyer Valley suggest that $^{87}Sr/^{86}Sr$ is a useful isotopic fingerprinting tool to determine the source aquifers of stream baseflow and groundwater-dependant ecosystems.

6. Conclusions

In this study, we have developed a systematic Sr isotope ($^{87}Sr/^{86}Sr$) fingerprinting framework of rocks and water in a complex multi-aquifer and aquitard system hosted within economically important adjoining coal- and gas-bearing sedimentary basins and overlying alluvial aquifers and streams in eastern Australia (Surat Basin and Clarence-Moreton basins, SCM basins). This confirmed that Sr isotopes are a powerful fingerprinting tool to enhance confidence in bore aquifer assignments and underpin identification of plausible aquifer and surface water interconnection pathways.

The confirmation of formation-characteristic whole rock $^{87}Sr/^{86}Sr$ provided the foundation for an in-depth assessment of groundwater $^{87}Sr/^{86}Sr$. Although the overall range of groundwater $^{87}Sr/^{86}Sr$ is lower than that of the whole rock $^{87}Sr/^{86}Sr$, the relative differences for groundwater $^{87}Sr/^{86}Sr$ are similar for groundwater, and the ratios also show statistically significant variability for different formations. The comparison with selected hydrochemical and groundwater age tracers (Carbon-14 and Chlorine-36) suggests only limited changes of $^{87}Sr/^{86}Sr$ from recharge beds to the deeper parts of the basins or with a decrease in natural Carbon-14 and Chlorine-36 tracer content along the flow paths. This indicates that the $^{87}Sr/^{86}Sr$ in these formations evolves early along the flow path and that the likelihood of incorporating new Sr is reduced unless there is a very soluble lithology.

The $^{87}Sr/^{86}Sr$ of the Walloon Coal Measures rocks and groundwaters is very different from over- and underlying sedimentary aquifers (Springbok Sandstone and Hutton Sandstone). This suggests that the $^{87}Sr/^{86}Sr$ are a powerful tool to support groundwater management through the assessment of potential inter-aquifer leakage due to water extraction from the Walloon Coal Measures for CSG production and an increased confidence of aquifer association for groundwater bores. The initial identification of systematic contrasts in whole-rock and groundwater $^{87}Sr/^{86}Sr$ in major aquifers resulted in implementation of routine $^{87}Sr/^{86}Sr$ monitoring as part of the regulatory framework in the SCM basins by the Office of Groundwater Impact Assessment (OGIA).

The assessment of whole rock $^{87}Sr/^{86}Sr$ also provides a tool for chemostratigraphy within the SCM basins. Despite considerable advancements in understanding the geology and hydrogeology of the SCM basins over the last decade, multiple geological boundaries (both vertical boundaries between aquifers and horizontal surface geology boundaries) remain uncertain in some areas of the basins. This study confirmed that together with other indicators, $^{87}Sr/^{86}Sr$ ratios of rocks can provide an additional line of evidence to refine the stratigraphy and geology of the SCM basins.

The comparison of surface water and groundwater $^{87}Sr/^{86}Sr$ in the Lockyer Valley, a major agricultural catchment within the SCM basins, confirmed that Sr isotopes are also useful to determine the source aquifer of groundwater-dependent ecosystems such as streams.

Applying the methods used in this study to local or regional hydrogeological connectivity investigations within the SCM basins, other sedimentary basins in Australia, and globally, can help to constrain three- and four-dimensional conceptual aquifer models and facilitate improved management of water resources. However, as the systematics of $^{87}Sr/^{86}Sr$ in rocks, groundwater and surface water are regionally and geologically specific, it is important to follow a sequential workflow which involves an initial assessment to determine if there is a contrast in the difference between $^{87}Sr/^{86}Sr$ of strata in different formations. If this difference is observed, it is appropriate to proceed to determine if there is a variability in sedimentary bedrock groundwater samples in these formations and compare them with other complementary tracers.

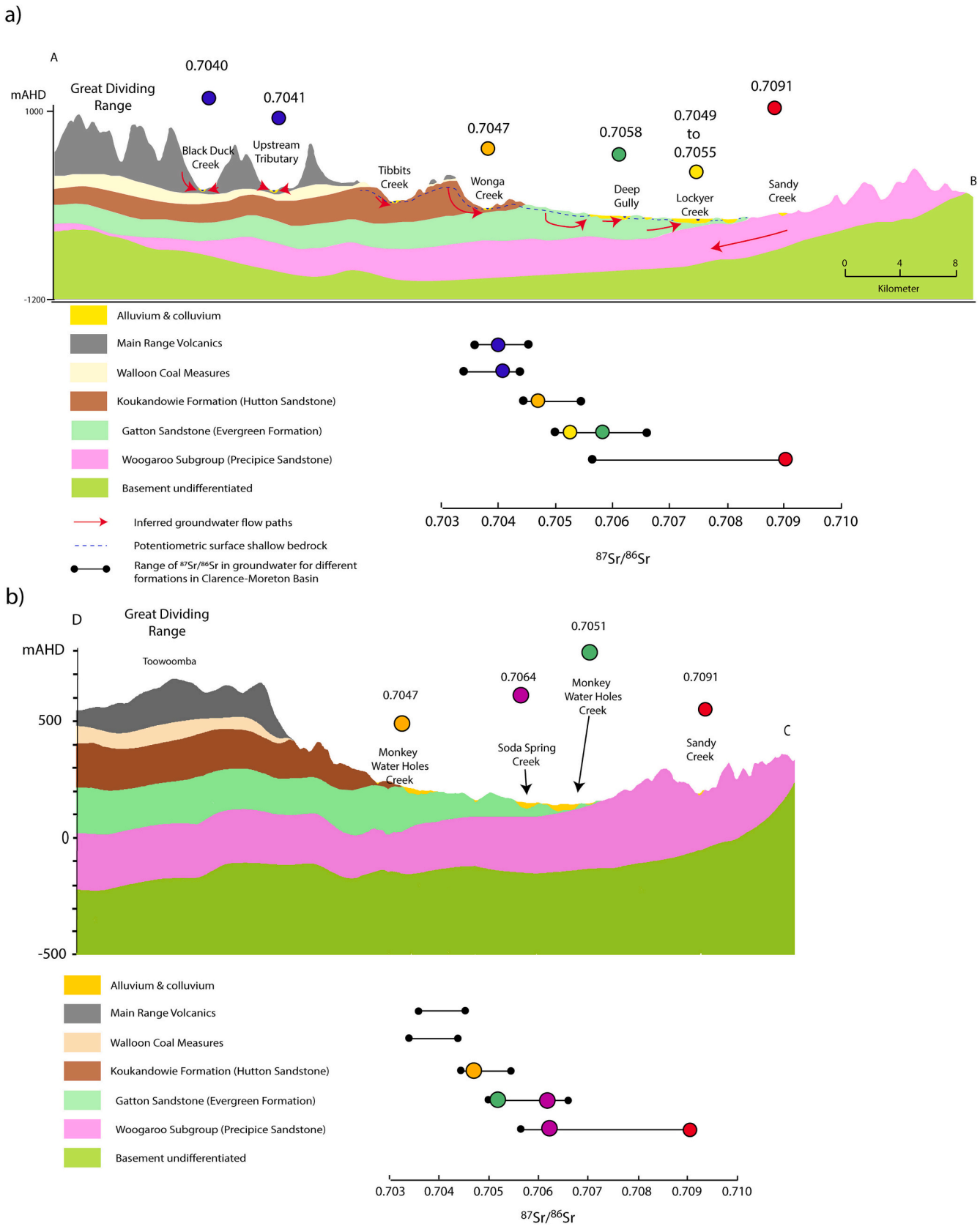

Fig. 10. $^{87}Sr/^{86}Sr$ of surface water systems along selected cross-sections through the Lockyer Valley based on the 3D geological model by Raiber et al. (2019). The orientations of the cross-sections are shown in Fig. 9. The coloured circles on the $^{87}Sr/^{86}Sr$ range bars indicate from which aquifer stream water is most likely sourced.

CRediT authorship contribution statement

M. Raiber: Writing – original draft, Visualization, Methodology, Investigation, Funding acquisition, Formal analysis, Data curation, Conceptualization. **A.J. Feitz:** Writing – review & editing, Methodology, Investigation, Funding acquisition, Formal analysis, Data curation, Conceptualization. **S. Flook:** Writing – review & editing, Investigation, Funding acquisition, Formal analysis. **D.I. Cendón:** Writing – review & editing, Investigation, Formal analysis, Data curation. **A. Suckow:** Writing – review & editing, Investigation, Funding acquisition, Formal analysis, Data curation. **G. Schöning:** Writing – review & editing, Software, Investigation, Funding acquisition, Data curation. **H. Hofmann:** Writing – review & editing, Investigation, Funding acquisition, Formal analysis, Data curation. **J. Martinez:** Writing – review & editing, Investigation, Funding acquisition, Data curation. **R. Maas:** Writing – review & editing, Methodology, Investigation, Formal analysis, Data curation. **B.F.J. Kelly:** Writing – review & editing, Funding acquisition, Formal analysis, Data curation.

Declaration of competing interest

The authors declare that they have no known financial interest or personal relationship that could have appeared to influence the work reported in this paper.

Data availability

All data are attached in Appendix A and C

Acknowledgements

This publication integrates data collected between 2011 and 2022 as part of multiple independent research projects by authorship team members from different organisations and with funding provided to different organisations from multiple sources.

Funding to this research was provided through CSIRO's Gas Industry Social and Environmental Research Alliance (GISERA) with contributions from the Australian Government's Department of Industry, Science and Resources. GISERA is a collaboration between CSIRO, Commonwealth, state and territory governments and industry established to undertake research on the impacts of onshore gas exploration and development on the environment, and the socio-economic costs and benefits. For information about GISERA's governance structure, projects and research findings visit https://gisera.csiro.au. This research was also supported through CSIRO strategic funding.

The Queensland Office of Groundwater Impact Assessment (OGIA) was established in 2011 to undertake independent cumulative impact assessments of coal seam gas (CSG), conventional oil and gas, and mining activities, focusing on the Surat, Clarence-Moreton and southern Bowen basins. Technical assessments and management arrangements are revised every three years and reported in an Underground Water Impact Report. OGIA is funded by a levy on resource tenure holders (https://www.ogia.water.qld.gov.au/about).

Funding to the University of New South Wales for collection and analysis of alluvial samples in the Condamine River catchment was provided by the Cotton Research and Development Corporation (CRDC), Australia, Grant Number UNSW1401. The authors would like to thank Charlotte Iverach and Lucienne Martel for their assistance with sample collection.

An ANSTO Research Portal Proposal Grant AP12150 to the University of Queensland, ANSTO and CSIRO ("Finding the Edge – Using environmental tracers to assess inter-basin connectivity between the Surat and Clarence-Moreton basins and define the eastern margin of the Great Artesian Basin") is gratefully acknowledged.

A small subset of samples was collected and analyzed in 2022 as part of Geoscience Australia's project 'Assessing the Status of Groundwater in the Great Artesian Basin', and the authors gratefully acknowledge funding provided through the Australian Government National Water Infrastructure Development Fund to conduct this research. Streamline Hydro are thanked for their assistance with sample collection and logistics for this project.

A postdoctoral research fellowship to MR by Queensland University of Technology (QUT) and the National Centre for Groundwater Research and Training (NCGRT) is gratefully acknowledged.

The Queensland Core Library (Exploration Data Centre, Zellmere, Queensland Department of Resources) is gratefully acknowledged for providing access to core (rock) samples.

The authorship team of this paper would like to thank the Queensland Department of Regional Development, Manufacturing and Water (RDMW), councils, private landholders, and CSG tenure holders Arrow Energy, QGC, Origin Energy and Santos and their groundwater teams within the Surat and Clarence-Moreton basins for access to groundwater bores, sharing local knowledge, and field and logistical support during groundwater sampling. The authors would also like to thank Santos for their help with spring sample collection in the Surat Basin.

Clément Duvert is thanked for providing unpublished data on Sr concentrations in the Teviot Brook catchment.

Jodie Pritchard (CSIRO) and Cornelia Wilske (CSIRO and University of Adelaide) are thanked for providing very useful review comments that have improved the manuscript.

Sonja Chandler is thanked for editing of the manuscript.

Supplementary data

Supplementary data to this article can be found online at https://doi.org/10.1016/j.scitotenv.2024.175522.

References

ABS (Australian Bureau of Statistics), 2020. Value of agricultural commodities produced. https://www.abs.gov.au/methodologies/value-agricultural-commodities-produced-australia-methodology/2018-19. (Accessed 4 February 2021).

Adams, S., Gruen, R., McGahan, D., et al., 2019. A strontium isoscape of north-east Australia for human provenance and repatriation. Geoarchaeology 34 (3), 231–251. https://doi.org/10.1002/gea.21728.

Anderson, T.T., Bestland, E.A., Wallis, I., et al., 2021. Catchment-scale groundwater-flow and recharge paradox revealed from base flow analysis during the Australian Millennium Drought (Mt Lofty Ranges, South Australia). Hydrogeol. J. https://doi.org/10.1007/s10040-020-02281-0.

Bagheri, R., Nadri, A., Raeisi, E., Eggenkamp, H.G.M., Kazemi, G.A., Montaseri, A., 2014. Hydrochemical and isotopic ($\delta^{18}O$, $\delta^{2}H$, $^{87}Sr/^{86}Sr$, $\delta^{37}Cl$ and $\delta^{81}Br$) evidence for the origin of saline formation water in a gas reservoir. Chem. Geol. 384, 62–75. https://doi.org/10.1016/j.chemgeo.2014.06.017.

Bataille, C.P., von Holstein, I., Laffoon, J.E., Willmes, M., Liu, X.M., Davies, G.R., 2018. A bioavailable strontium isoscape for Western Europe: a machine learning approach. PLoS One 13 (5), e0197386. https://doi.org/10.1371/journal.pone.0197386.

Bataille, C.P., Crowley, B.E., Wooller, M.J., Bowen, G.J., 2020. Advances in global bioavailable strontium isoscapes. Palaeogeogr. Palaeoclimatol. Palaeoecol. 555 https://doi.org/10.1016/j.palaeo.2020.109849.

Baublys, K.A., Hamilton, S.K., Golding, S.D., Vink, S., Esterle, J., 2015. Microbial controls on the origin and evolution of coal seam gases and production waters of the Walloon Subgroup; Surat Basin, Australia. Int. J. Coal Geol. 147–148, 85–104. https://doi.org/10.1016/j.coal.2015.06.007.

Baublys, K.A., Hamilton, S.K., Hofmann, H., Golding, S.D., 2019. A strontium ($^{87}Sr/^{86}Sr$) isotopic study on the chemical evolution and migration of groundwaters in a low-rank coal seam gas reservoir (Surat Basin, Australia). Appl. Geochem. 101, 1–18. https://doi.org/10.1016/j.apgeochem.2018.12.020.

Baublys, K.A., Hofmann, H., Esterle, J.S., Cendón, D.I., Vink, S., Golding, S.D., 2021. Geochemical influences on methanogenic groundwater from a low rank coal seam gas reservoir: Walloon Subgroup, Surat Basin. Int. J. Coal Geol. 246, 103841 https://doi.org/10.1016/j.coal.2021.103841.

Bianchi, V., Pistellato, D., Job, A., Esterle, J., 2019. Regional Geological Study of the Hutton Sandstone. ANLEC 7-1116-0294 Final Report. University of Queensland, Brisbane.

Bradshaw, B.E., Spencer, L.K., Lahtinen, A.C., Khider, K., Ryan, D.J., Colwell, J.B., Chirinos, A., Bradshaw, J., 2009. Queensland Carbon Dioxide Geological Storage Atlas. Queensland Department of Employment, Economic Development and Innovation, Brisbane.

de Caritat, P., Dosseto, A., Dux, F., 2022. A strontium isoscape of inland southeastern Australia. Earth System Science Data 14, 4271–4286. https://doi.org/10.5194/essd-14-4271-2022.

Chapman, E.C., Capo, R.C., Stewart, B.W., Kirby, C.S., Hammack, R.W., Schroeder, K.T., Edenborn, H.M., 2012. Geochemical and strontium isotope characterization of produced waters from Marcellus shale natural gas extraction. Environ. Sci. Technol. 2012, 3545–3553. https://doi.org/10.1021/es204005g.

Cohen, B.E., Withnall, I.W., Vasconcelos, P.M., 2013. Intraplate magmatism of eastern Queensland. In: Jell, P.A. (Ed.), Geology of Queensland. Geological Survey of Queensland, Brisbane, pp. 629–645.

Collerson, K., Ullman, W., Torgersen, T., 1988. Ground waters with unradiogenic $^{87}Sr/^{86}Sr$ ratios in the Great Artesian Basin. Australia. Geology 16 (1), 59–63. https://doi.org/10.1130/0091-7613(1988)016%3C0059:GWWUSS%3E2.3.CO;2.

Cook, A.G., Bryan, S.E., Draper, J., 2013. Post-orogenic Mesozoic basins and magmatism. In: Jell, P. (Ed.), Geology of Queensland. Geological Survey of Queensland, Brisbane, pp. 515–571.

Crosbie, R.S., Raiber, M., Wilkins, A., Dawes, W., Louth-Robins, T., Gao, L., 2022. Quantifying Diffuse Recharge to the Great Artesian Basin Groundwater System. CSIRO, Australia. https://doi.org/10.25919/waky-s739.

Cui, T., Raiber, M., Pagendam, D., Gilfedder, M., Rassam, D., 2018. Response of groundwater level and surface-water/groundwater interaction to climate variability: Clarence-Moreton Basin, Australia. Hydrogeol. J. 26, 593–614. https://doi.org/10.1007/s10040-017-1653-6.

DNRME (Queensland Department of Natural Resources, Mines and Energy), 2020. Qld groundwater database. https://www.data.qld.gov.au/dataset/groundwater-database-queensland.

Doig, A., Stanmore, P., 2012. The Clarence-Moreton Basin in New South Wales; geology, stratigraphy and coals seam gas characteristics. In: Eastern Australasian Basins Symposium IV. Brisbane, Queensland, pp. 71–84.

Donchak, P.J.T., Purdy, D.J., Denaro, T.J., Bultitude, R.J., 2007. Geology and Mineralisation of the Texas Region. South-east Queensland, Geological Survey Office, Queensland Department of Mines and Energy.

Dromagaci, S.S., Herczeg, A.L., 2002. Strontium and carbon isotope constraints on carbonate-solution interactions and inter-aquifer mixing in groundwaters of the semi-arid Murray Basin, Australia. J. Hydrol. 262, 50–67. https://doi.org/10.1016/S0022-1694(02)00021-5.

Duvert, C., Raiber, M., Owen, D.D.R., Cendón, D.I., Batiot-Guilhe, C., Cox, M.E., 2015. Hydrochemical processes in a shallow coal seam gas aquifer and its overlying stream–alluvial system: implications for recharge and inter-aquifer connectivity. Appl. Geochem. 61, 146–159. https://doi.org/10.1016/j.apgeochem.2015.05.021.

Erasmus, D., Flook, S., Foster, L., Gallagher, M., Bui Xuan Hy, A., Lowry, S., Beck, D., Pandey, S., 2024. Methodology for the assignment of aquifers to bores in the Surat and southern Bowen basins. accessed from, Qld Office of Groundwater Impact Assessment. https://www.ogia.water.qld.gov.au/publications-reports (34 pages).

Ewart, A., Chappell, B.W., Menzies, M.A., 1988. An overview of the geochemical and isotopic characteristics of the eastern Australian Cainozoic volcanic provinces. J. Petrol. 1, 225–273. https://doi.org/10.1093/petrology/Special_Volume.1.225.

Exon, N.F., 1976. Geology of the Surat Basin in Queensland. Bur. Miner. Resour. Geol. Geophys. Bull. 166. https://d28rz98at9flks.cloudfront.net/77/Bull_166.pdf.

Farquhar, S.M., Dawson, G.K.W., Esterle, J.S., Golding, S.D., 2013. Mineralogical characterisation of a potential reservoir system for CO_2 sequestration in the Surat Basin. Aust. J. Earth Sci. 60, 91–110. https://doi.org/10.1080/08120099.2012.752406.

Faure, G., Powell, J.L., 2012. Strontium Isotope Geology, vol. 5. Springer Science & Business Media.

Feitz, A., Ransley, T., Hodgkinson, J., Preda, M., Dunsmore, D., McKillop, J., Spulak, R., Dixon, O., Kuske, T., Draper, J., 2014. GA-GSQ Hydrochemistry Dataset (2009–2011), GEOCAT No. 78549. Geoscience Australia, Canberra, Australia. https://pid.geoscience.gov.au/dataset/ga/78549.

Fielding, C.R., 1993. The Middle Jurassic Walloon Coal Measures in the type area, the Rosewood-Walloon coalfield, SE Queensland. Aust. Coal Geol. 9, 4–16.

Fifield, L.K., 1999. Accelerator mass spectrometry and its applications. Rep. Prog. Phys. 62, 1223–1274.

Fifield, L.K., Tims, S.G., Stone, J.O., Argento, D.C., De Cesare, M., 2013. Ultra-sensitive measurements of ^{36}Cl and ^{236}U at the Australian National University. Nuclear Instruments and Methods in Physics B 294, 126–131. https://doi.org/10.1016/j.nimb.2012.04.028.

Fink, D., Hotchkis, M., Hua, Q., Jacobsen, G., Smith, A.M., Zoppi, U., Child, D., Mifsud, C., van der Gaast, H., Williams, A., Williams, M., 2004. The ANTARES AMS Facility at ANSTO, Nuclear Instruments and Methods in Physics Research Section B: Beam Interactions With Materials and Atoms, vol. 223–224, pp. 109–115. https://doi.org/10.1016/j.nimb.2004.04.025.

Flook, S., Fawcett, J., Cox, R., Pandey, S., Schoening, G., Khor, J., Singh, D., Suckow, A., Raiber, M., 2020. A multidisciplinary approach to the hydrological conceptualisation of springs in the Surat Basin of the Great Artesian Basin (Australia). Hydrogeol. J. 28, 219–236. https://doi.org/10.1007/s10040-019-020.

Frost, C., Pearson, B., Ogle, K., Heffern, E., Lyman, R., 2002. Sr isotope tracing of aquifer interactions in an area of accelerating coal-bed methane production, Powder River Basin, Wyoming. Geology 30, 923–926. https://doi.org/10.1130/0091-7613(2002)030%3C0923:SITOAI%3E2.0.CO;2.

Green, P.M., Carmichael, D.C., Brain, T.J., Murray, C.G., McKellar, J.L., Beeston, J.W., Gray, A.R.G., 1997. Lithostratigraphic units in the Bowen and Surat Basins, Queensland. In: Green, P.M. (Ed.), The Surat and Bowen Basins, South-east Queensland, Queensland Minerals and Energy Review Series, Queensland Geological Survey, Brisbane, vol. 1, pp. 41–108.

Guiton, S., Kieft, R., Churchill, J., Sheerin, C., 2015. Characterising the Hutton Sandstone in the Northeastern Surat Basin. In: AAPG Asia Pacific Region, Geoscience Technology Workshop, Opportunities in Coal Bed Methane in the Asia Pacific. Australia, AAPG, Brisbane.

Gwynne, R., Frape, S., Shouakar-Stash, O., Love, A., 2013. ^{81}Br, ^{37}Cl, and ^{87}Sr studies to assess groundwater flow and solute sources in the southwestern Great Artesian Basin. Australia, Procedia Earth and Planetary Science 7, 330–333. https://doi.org/10.1016/j.proeps.2013.03.084.

Harkness, J.S., Darrah, T.H., Warner, N.R., Whyte, C.J., Moore, M.T., Millot, R., Kloppmann, W., Jackson, R.B., Vengosh, A., 2017. The geochemistry of naturally occurring methane and saline groundwater in an area of unconventional shale gas development. Geochim. Cosmochim. Acta 208, 302–334. https://doi.org/10.1016/j.gca.2017.03.039.

Harrington, G.A., Herczeg, A.L., 2003. The importance of silicate weathering of a sedimentary aquifer in arid Central Australia indicated by very high $^{87}Sr/^{86}Sr$ ratios. Chem. Geol. 199 (3–4), 281–292. https://doi.org/10.1016/S0009-2541(03)00128-1.

Hayes, P., Nicol, C., La Croix, A.D., Pearce, J., Gonzalez, S., Wang, J., Harfoush, A., He, J., Moser, A., Helm, L., Morris, R., Gornall, D., 2020. Enhancing geological and hydrogeological understanding of the Precipice Sandstone aquifer of the Surat Basin, Great Artesian Basin, Australia, through model inversion of managed aquifer recharge datasets. Hydrogeol. J. 28, 175–192. https://doi.org/10.1007/s10040-019-02079-9.

Helsel, D.R., Hirsch, R.M., 2002. Statistical methods in water resources. In: Techniques of Water-resources Investigations of the United States Geological Survey. Book 4, Hydrologic Analysis and Interpretation (524 pp.).

Herut, B., Starinsky, A., Katz, A., 1993. Strontium in rainwater from Israel: sources, isotopes and chemistry. Earth Planet. Sci. Lett. 120, 77–84. https://ui.adsabs.harvard.edu/link_gateway/1993E&PSL.120...77H/doi:10.1016/0012-821X(93)90024-4.

Hofmann, H., Cartwright, I., 2013. Using hydrogeochemistry to understand inter-aquifer mixing in the on-shore part of the Gippsland Basin, southeast Australia. Appl. Geochem. 33, 84–103. https://doi.org/10.1016/j.apgeochem.2013.02.004.

Hofmann, H., Pearce, J.K., Hayes, P., Golding, S.D., Hall, N., Baublys, K.A., Raiber, M., Suckow, A., 2024. Multi-tracer approach to constrain groundwater flow and geochemical baseline assessments for CO_2 sequestration in deep sedimentary basins. Int. J. Coal Geol., 104438 https://doi.org/10.1016/j.coal.2023.104438.

Horner, K.N., Schacht, U., Haese, R.R., 2015. Characterizing long-term CO_2–water–rock reaction pathways to identify tracers of CO_2 migration during geological storage in a low-salinity, siliciclastic reservoir system. Chem. Geol. 399, 123–133. https://doi.org/10.1016/j.chemgeo.2014.09.021.

Ingram, F.T., Robinson, V.A., 1996. Petroleum prospectivity of the Clarence-Moreton Basin in New South Wales. In: Facer, R.A. (Ed.), Petroleum Bulletin 3. New South Wales Department of Mineral Resources.

Iverach, C., Cendón, D., Hankin, S., Lowry, D., Fisher, R.E., France, J.L., Nisbet, E.G., Baker, A., Kelly, B.F.J., 2015. Assessing connectivity between an overlying aquifer and a coal seam gas resource using methane isotopes, dissolved organic carbon and tritium. Sci. Rep. 5, 15996 https://doi.org/10.1038/srep15996.

Jackson, M.G., Hart, S.R., 2006. Strontium isotopes in melt inclusions from Samoan basalts: implications for heterogeneity in the Samoan plume. Earth Planet. Sci. Lett. 245, 260–277. https://doi.org/10.1016/j.epsl.2006.02.040.

Jenkinson, L.G., 2018. Approaches to Fines Production in the Walloons Subgroup, Surat Basin, Queensland. University of Adelaide, Australian School of Petroleum (Thesis (MPhil), 2018, 143 p.).

King, A.C., Raiber, M., Céndon, D.I., Cox, M.E., Hollins, S.E., 2015. Identifying flood recharge and inter-aquifer connectivity using multiple isotopes in subtropical Australia. Hydrol. Earth Syst. Sci. 19 (5), 2315–2335. https://doi.org/10.5194/hess-19-2315-2015.

Korsch, R.J., O'Brien, P.E., Sexton, M.J., Wake-Dyster, K.D., Wells, A.T., 1989. Development of Mesozoic transtensional basins in easternmost Australia. Aust. J. Earth Sci. 36 (1), 13–28. https://doi.org/10.1080/14400958908527948.

Kossert, K., 2003. Half-life measurements of ^{87}Rb by liquid scintillation counting. Appl. Radiat. Isot. 59 (5–6), 377–382. https://doi.org/10.1016/j.apradiso.2003.08.004.

La Croix, A.D., Wang, J., He, J., Hannaford, C., Bianchi, V., Esterle, J., Undershultz, J.R., 2019. Widespread nearshore and shallow marine deposition within the Lower Jurassic Precipice Sandstone and Evergreen Formation in the Surat Basin, Australia. Mar. Pet. Geol. 109, 760–790. https://doi.org/10.1016/j.marpetgeo.2019.06.048.

La Croix, A.D., He, J., Bianchi, V., Wang, J., Gonzalez, S., Underschultz, J.R., 2020. Early Jurassic palaeoenvironments in the Surat Basin, Australia – marine incursion into eastern Gondwana. Sedimentology 67, 457–485. https://doi.org/10.1111/sed.12649.

La Croix, A.D., Sobczak, K., Esterle, J.S., Bianchi, V., Wang, J., He, J., Hayes, P., Underschultz, J.R., Garnett, A., 2022. Integrating palynostratigraphy with zircon geochronology in the Lower Jurassic Precipice Sandstone and Evergreen Formation to improve stratigraphic correlation within the Great Artesian Basin, Australia. Mar. Pet. Geol. 144, 105845 https://doi.org/10.1016/j.marpetgeo.2022.105845.

Lemarchand, D., Jacobson, A.D., Cividini, D., Chabaux, F., 2015. The major ion, $^{87}Sr/^{86}Sr$, and $\delta^{11}B$ geochemistry of groundwater in the Wyodak-Anderson coal bed aquifer (Powder River Basin, Wyoming, USA). Compt. Rendus Geosci. 347 (7–8) https://doi.org/10.1016/j.crte.2015.05.007.

Li, H., Lau, Hon Chung, Huang, Shan, 2018. China's coalbed methane development: a review of the challenges and opportunities in subsurface and surface engineering. J. Pet. Sci. Eng. 166, 621–635. https://doi.org/10.1016/j.petrol.2018.03.047 (ISSN 0920-4105).

Maas, R., Grew, E.S., Carson, C.J., 2015. Isotopic constraints (Pb, Rb-Sr, Sm-Nd) on the sources of Early Cambrian pegmatites with boron and beryllium minerals in the Larseman Hills, Prydz Bay, Antarctica. Can. Mineral. 53, 249–272. https://doi.org/10.3749/canmin.1400081.

Mallants, D., Raiber, M., Davies, P., 2016. Decision Support System for Investigating Gas in Water Bores and Links to Coal Seam Gas Development. Project Report Prepared

for the Department of Natural Resources and Mines, Queensland. https://doi.org/10.13140/RG.2.2.11038.74561.
Martin, M.A., Wakefield, M., MacPhail, M.K., Pearce, T., Edwards, H.E., 2013. Sedimentology and stratigraphy of an intra-cratonic basin coal seam gas play: Walloon Subgroup of the Surat Basin, eastern Australia. Pet. Geosci. 19, 21–38. https://doi.org/10.1144/petgeo2011-043.
Martinez, J., Raiber, M., Cox, M.E., 2015. Assessment of groundwater-surface interaction via combination of long-term hydrochemical dataset and isotope hydrology: an example from the headwaters of the Condamine River, Southeast Queensland, Australia. Sci. Total Environ. 536, 499–516. https://doi.org/10.1016/j.scitotenv.2015.07.031.
McNutt, R.H., 2000. Strontium isotopes. In: Cook, P.G., Herczeg, A.L. (Eds.), Environmental Tracers in Subsurface Geology. Kluwer, Boston, pp. 234–260.
Moya, C.E., Raiber, M., Taulis, M., Cox, M.E., 2016. Using environmental isotopes to constrain hydrochemical processes and inter-aquifer mixing in the Galilee and Eromanga basins, Great Artesian Basin, Australia. J. Hydrol. 539, 304–318. https://doi.org/10.1016/j.jhydrol.2016.05.016.
Mukherjee, S., Rajabi, M., Esterle, J., 2021. Relationship between coal composition, fracture abundance and initial reservoir permeability: a case study in the Walloon Coal Measures, Surat Basin. Australia. International Journal of Coal Geology 240, 103726. https://doi.org/10.1016/j.coal.2021.103726.
Négrel, P., Casanova, J., Aranyossy, J.F., 2001. Strontium isotope systematics used to decipher the origin of groundwaters sampled from granitoids: the Vienne Case (France). Chem. Geol. 177 (3–4), 287–308. https://doi.org/10.1016/S0009-2541(00)00414-9.
Négrel, P., Guerrot, C., Millot, R., 2007. Chemical and strontium isotope characterization of rainwater in France: influence of sources and hydrogeochemical implications. Isot. Environ. Health Stud. 43, 179–196. https://doi.org/10.1080/10256010701550773.
Négrel, P., Petelet-Giraud, E., Millot, R., 2017. Sr isotopes as mixing and lithological tracers; the Ebro River Basin. Procedia Earth Planet. Sci. 17, 782–785. https://doi.org/10.1016/j.proeps.2017.01.028.
Neymark, L.A., Premo, W.R., Emsbo, P., 2018. Combined radiogenic ($^{87}Sr/^{86}Sr$, $^{234}U/^{238}U$) and stable ($\delta^{88}Sr$) isotope systematics as tracers of anthropogenic groundwater contamination within the Williston Basin, USA. Appl. Geochem. 96, 11–23. https://doi.org/10.1016/j.apgeochem.2018.06.006.
O'Brien, P.E., Wells, A.T., 1994. Sedimentology of the Bundamba Group, Clarence-Moreton Basin. In: Wells, A.T., O'Brien, P.E. (Eds.), Geology and Petroleum Potential of the Clarence-Moreton Basin, New South Wales and Queensland, Australian Geological Survey Organisation, Bulletin, vol. 241, pp. 72–138.
OGIA, 2016. Hydrogeological conceptualisation report for the Surat Cumulative Management Area. accessed from, Qld Office of Groundwater Impact Assessment. https://www.ogia.water.qld.gov.au/publications-reports (405 pages).
OGIA, 2021a. A summary of Underground Water Impact Report 2021 for the Surat Cumulative Management Area. accessed from, Qld Office of Groundwater Impact Assessment. https://www.ogia.water.qld.gov.au/publications-reports (20 pages).
OGIA, 2021b. Geology and 3D geological models for Queensland's Surat and southern Bowen basins – stratigraphic framework, data, methods and results. accessed from, Qld Office of Groundwater Impact Assessment. https://www.ogia.water.qld.gov.au/publications-reports.
OGIA, 2023. Analysis of groundwater trends to identify impacts from coal seam gas and coal mining in the Surat and southern Bowen basins (OGIACD14V1). accessed from. https://www.rdmw.qld.gov.au/_data/assets/pdf_file/0007/1661884/analysis-groundwater-trends-impacts-csg-coal-mining.pdf.
Palmer, M.R., Edmond, J.M., 1989. The strontium isotope budget of the modern ocean. Earth Planet. Sci. Lett. 92, 11–26. https://doi.org/10.1016/0012-821X(89)90017-4.
Pandey, S., Dhananjay, S., Denner, S., Cox, R., Herbert, S., Dickinson, C., Gallagher, M., Foster, L., Cairns, B., Gossmann, S., 2020. Inter-aquifer connectivity between Australia's Great Artesian Basin and the overlying Condamine Alluvium: an assessment and its implications for the basin's groundwater management. Hydrogeol. J. 28, 125–146. https://doi.org/10.1007/s10040-019-02089-7.
Pearce, J.K., Golding, S.D., Baublys, K.A., Hofmann, H., Cendón, D.I., Herbert, St.J., Hayes, P.J., 2022. Multiple tracers for dis-connectivity of shallow aquifers, alluvium, and coal seam gas wells in the Great Artesian Basin. The APPEA Journal 62, S480–S486. https://doi.org/10.1071/AJ21082.
Petelet-Giraud, E., Négrel, P., Casanova, J., 2018. Tracing surface water mixing and groundwater inputs using chemical and isotope fingerprints ($\delta^{18}O$-$\delta^{2}H$, $^{87}Sr/^{86}Sr$) at basin scale: the Loire River (France). Appl. Geochem. 97, 279–290. https://doi.org/10.1016/j.apgeochem.2018.08.028.
Peucker-Ehrenbrink, B., Fiske, G.J., 2019. A continental perspective of the seawater $^{87}Sr/^{86}Sr$ record: a review. Chem. Geol. 510, 140–165. https://doi.org/10.1016/j.chemgeo.2019.01.017 (ISSN 0009-2541).
Phan, T.T., Gardiner, J.B., Capo, R.C., Stewart, B.W., 2018. Geochemical and multi-isotopic ($^{87}Sr/^{86}Sr$, $^{143}Nd/^{144}Nd$, $^{238}U/^{235}U$) perspectives of sediment sources, depositional conditions, and diagenesis of the Marcellus Shale. Appalachian Basin, USA, Geochimica et Cosmochimica Acta 222, 187–211. https://doi.org/10.1016/j.gca.2017.10.021.
Raiber, M., Suckow, A., 2017. Hydrochemical Assessment of the Hutton and Precipice Sandstones in the Northern Surat Basin. CSIRO, Australia.
Raiber, M., Webb, J.A., Bennetts, D.A., 2009. Strontium isotopes as tracers to delineate aquifer interactions and the influence of rainfall in the Basalt Plains of southeastern Australia. J. Hydrol. 367 (3–4), 188–199. https://doi.org/10.1016/j.jhydrol.2008.12.020.
Raiber, M., Cendón, D, Feitz, A., Sundaram, B. & Suckow, A., 2014. Hydrochemical and isotopic fingerprinting of the Walloon Coal Measures and adjacent aquifers in the Clarence-Moreton and eastern Surat basins in southeast Queensland. Australian Earth Science Convention, Newcastle, July, 2014, 22nd Geological Convention, Newcastle NSW, 7–10 July 2014, 176–177.
Raiber, M., Murray, J., Bruce, C., Rassam, D., Ebner, B., Henderson, B., O'Grady, T., Gilfedder, M., Cui, T., Crosbie, R., Hartcher, M., 2017. Conceptual modelling for the Clarence-Moreton bioregion. Product 2.3 from the Clarence-Moreton Bioregional Assessment, Department of the Environment, Bureau of Meteorology, CSIRO and Geoscience Australia. http://data.bioregionalassessments.gov.au/product/CLM/CLM/2.3.
Raiber, M., Lewis, S., Cendón, D.I., Cui, T., Cox, M.E., Gilfedder, M., Rassam, D.W., 2019. Significance of the connection between bedrock, alluvium and streams: a spatial and temporal hydrogeological and hydrogeochemical assessment from Queensland, Australia. J. Hydrol. 569, 666–684. https://doi.org/10.1016/j.jhydrol.2018.12.020.
Raiber, M., Suckow, A., Deslandes, A., Gerber, C., Martinez, J., Crane, P., Ransley, T., Evans, T., Wallace, L., Wu, G., 2022. Assessing Recharge Processes and Flow Dynamics Using Environmental Tracers in the Great Artesian Basin. EP2022-5860. CSIRO, Australia. https://doi.org/10.25919/kb99-x235.
Ransley, T., Somerville, P., Tan, K.P., Feitz, A., Cook, S., Yates, G., Schoning, G., Bell, J., Caruana, L., Sundaram, B., Wallace, L., 2015. Groundwater hydrochemical characterisation of the Surat Region and Laura Basin – Queensland. In: Geoscience Australia, Canberra, Record 2015/05. https://doi.org/10.11636/Record.2015.005.
Scheiber, L., Cendón, D.I., Iverach, C.P., Hankin, S.I., Vázquez-Suñé, E., Kelly, B.F.J., 2020. Hydrochemical apportioning of irrigation groundwater sources in an alluvial aquifer. Sci. Total Environ. 744, 140506 https://doi.org/10.1016/j.scitotenv.2020.140506.
Smallacombe, J., Singh, D., Erasmus, D., Flook, S., Pandey, S., 2024. Water bores and groundwater use in the Surat and southern Bowen basins: a research update paper by the Office of Groundwater Impact Assessment (OGIA). accessed from. https://www.ogia.water.qld.gov.au/publications-reports (31 pages).
Sobczak, K., La Croix, A.D., Esterle, J., Hayes, P., Holl, H.-G., Ciesiolka, R., Crowley, J.L., Allen, C.M., 2022. Geochronology and sediment provenance of the Precipice Sandstone and Evergreen Formation in the Surat Basin, Australia: implications for the palaeogeography of eastern Gondwana. Gondwana Res. 111, 189–208. https://doi.org/10.1016/j.gr.2022.08.003 (ISSN 1342-937X).
Suckow, A., Taylor, A.R., Davies, P., Leaney, F.W., 2016. Geochemical Baseline Monitoring. Final Report, CSIRO, Australia. https://gisera.org.au/wp-content/uploads/2012/06/Project-4-GeochemicalBaseline-Report-201602.pdf.
Suckow, A., Raiber, M., Deslandes, A., Gerber, C., 2018. Constraining Conceptual Groundwater Models for the Hutton and Precipice Aquifers in the Surat Basin Through Tracer Data. Final Report, CSIRO, Australia. http://hdl.handle.net/102.100.100/87226?index=1.
Suckow, A., Deslandes, A., Raiber, M., Taylor, A.R., Davies, P., Gerber, C., Leaney, F., 2020. Reconciling contradictory environmental tracer ages in multi-tracer studies to characterize the aquifer and quantify deep groundwater flow: an example from the Hutton Sandstone, Great Artesian Basin, Australia. Hydrogeol. J. 28, 75–87. https://doi.org/10.1007/s10040-019-02042-8.
Suckow, A., Raiber, M., Martinez, J., Deslandes, A., Gerber, C., Mallants, D., 2021. Assessment of Connectivity of the Condamine Alluvium With the Walloon Coal Measures. An Environmental Tracer Pilot Study on Two Depth Profiles Using Noble Gases and Conventional Tracers to Gain Critical Information on Hydraulic Connectivity. CSIRO, Australia. https://doi.org/10.25919/tffk-jp93.
Sutherland, F.L., 2003. "Boomerang" migratory intraplate Cenozoic volcanism, eastern Australian rift margins and the Indian-Pacific mantle boundary. Geological Society of Australia Special Publication 22 and Geological Society of America Special Paper 372, 2003–2221. https://doi.org/10.1130/0-8137-2372-8.203.
Veizer, J., 1989. Strontium isotopes in seawater through time. Annu. Rev. Earth Planet. Sci. 17 (1), 141–167. https://doi.org/10.1146/annurev.ea.17.050189.001041.
Vink, S., Underschultz, J., Guiton, S., Xu, J., Honari, V., 2020. Flow system of the Hutton Sandstone in the northern Surat Basin, Australia. Hydrogeol. J. 28, 89–102. https://doi.org/10.1007/s10040-019-02097-7.
Wang, J., La Croix, A.D., Gonzalez, S., He, J., Underschultz, J., 2019. Sequence stratigraphic analysis of the Lower Jurassic Precipice Sandstone and Evergreen Formation in the Surat Basin, Australia: implications for the architecture of reservoirs and seals for CO_2 storage. Mar. Pet. Geol. 102, 829–843. https://doi.org/10.1016/j.marpetgeo.2019.01.038.
Wells, A.T., O'Brien, P.E., 1994. Lithostratigraphic framework of the Clarence-Moreton Basin. In: Wells, A.T., O'Brien, P.E. (Eds.), Geology and Petroleum Potential of the Clarence-Moreton Basin, New South Wales and Queensland, Australian Geological Survey Organisation, Bulletin, vol. 241, pp. 4–47.
Wilcken, K.M., Fink, D., Hotchkis, M.A.C., Garton, D., Button, D., Mann, M., Kitchen, R., Hauser, T., O'Connor, A., 2017. Accelerator mass spectrometry on SIRIUS: new 6 MV spectrometer at ANSTO. Nucl. Inst. Methods Phys. Res. B 406, 278–282. https://doi.org/10.1016/j.nimb.2017.01.003.
Williamson, T., Henderson, R.A., Price, G.D., Collerson, K.D., 2012. Strontium–isotope stratigraphy of the Lower Cretaceous of Australia. Cretac. Res. 36, 24–36. https://doi.org/10.1016/j.cretres.2012.02.001.